

Modeling CO₂ and water vapor turbulent flux distributions within a forest canopy

Chun-Ta Lai, Gabriel Katul, Ram Oren, David Ellsworth,¹ and Karina Schäfer

School of the Environment, Duke University, Durham, North Carolina

Abstract. One-dimensional multilayer biosphere-atmosphere models (e.g., CANVEG) describe ecosystem carbon dioxide (CO₂) and water vapor (H₂O) fluxes well when cold temperatures or the hydrologic state of the ecosystem do not induce stomatal closure. To investigate the CANVEG model framework under such conditions, CO₂, H₂O, and sensible heat fluxes were measured with eddy-covariance methods together with xylem sap flux and leaf-level gas exchange in a 16-year-old (in 1999) southeastern loblolly pine forest. Leaf-level gas exchange measurements, collected over a 3-year period, provided all the necessary biochemical and physiological parameters for the CANVEG model. Using temperature-induced reductions of the biochemical kinetic rate constants, the CANVEG approach closely captures the diurnal patterns of the CO₂ and H₂O fluxes for two different formulations of the maximum Rubisco catalytic capacity ($V_{c\max}$) – temperature function, suggesting that the CANVEG approach is not sensitive to $V_{c\max}$ variations for low temperatures. A soil moisture correction (w_r) to the Ball-Berry leaf-conductance approach was also proposed and tested. The w_r magnitude is consistent with values predicted by a root-xylem hydraulic approach and with leaf-level measurements. The w_r correction significantly improves the model's ability to capture diurnal patterns of H₂O fluxes for drought conditions. The modeled bulk canopy conductance (G_m) for pine foliage estimated from the CANVEG-modeled multilevel resistance values agreed well with canopy conductance (G_c) independently estimated from pine sap flux measurements. Detailed sensitivity analysis suggests that the leaf-level physiological parameters used in CANVEG are not static. The dynamic property of the conductance parameter, inferred from such sensitivity analysis, was further supported using 3 years of porometry measurements. The CANVEG model also reproduced basic biochemical processes as demonstrated by the agreement between modeled and leaf-level measured C_i/C_a , where C_i and C_a are the intercellular and atmospheric CO₂ concentration, respectively. The model estimated that vapor pressure deficit does not vary significantly within the canopy but that C_i/C_a varied by more than 15%. The broader implication of this variation is that “big-leaf” approaches that compress physiological and biochemical parameters into bulk canopy stomatal properties may be suitable for estimating water vapor flux but biased for CO₂ ecosystem fluxes.

1. Introduction

Coupling biophysical, physiological, and biochemical principles with detailed turbulent transport mechanics to estimate carbon dioxide (CO₂) and water vapor (H₂O) sources and sinks (hereinafter referred to as source) and flux distributions within a forest canopy offers a promising approach to model biosphere-atmosphere exchange from forested ecosystems. An example of such framework, termed CANVEG by *Baldocchi and Meyers* [1998], permits realistic accounting for the primary interdependencies between the vegetation and its microclimate. Models based on the CANVEG framework reproduced well measured scalar fluxes in several vegetation types [*Baldocchi and Harley*, 1995; *Baldocchi*, 1997; *Baldocchi et al.*, 1997a; *Baldocchi and Meyers*, 1998].

In current CANVEG models, velocity statistics, particularly the standard deviation of vertical velocity (σ_w) and Lagrangian integral timescales (T_L) within the canopy are assumed or heuristically specified [*Raupach*, 1988; *Baldocchi*, 1992; *Baldocchi and Meyers*, 1998]. In addition to being variable from stand to stand, the flow statistics also evolve with leaf area dynamics. Thus this approach prohibits using CANVEG for long-term flux estimation because the effects of variable leaf area density on the required flow statistics cannot be explicitly resolved. To circumvent these limitations, *Lai et al.* [2000] developed a CANVEG approach that includes a one-dimensional second-order Eulerian closure model to compute the velocity statistics within the canopy volume which are needed for estimating sources and fluxes. The CANVEG approach of *Lai et al.* [2000] has the added advantage of combining leaf area density distribution with mean momentum and Reynolds stress equations inside the canopy to infer first and second moments of the flow field. Thus the effects of variation in leaf area density on the flow statistics required for CO₂ and H₂O transport can be explicitly treated.

Over the past decade, many field experiments highlighted

¹Environmental Biology and Instrumentation Division, Brookhaven National Laboratory, Upton, New York.

Copyright 2000 by the American Geophysical Union.

Paper number 2000JD900468.
0148-0227/00/2000JD900468\$09.00

other limitations to the CANVEG approach. In particular, when soil moisture content (θ) or mean air temperature (T_a) are low enough to restrict stomatal opening [Hinckley et al., 1978; Gollan et al., 1986; Schulze, 1986; Kelliher et al., 1993; Cornic, 1994; Kramer and Boyer, 1995; Baldocchi et al., 1997b; Oren et al., 1998a; Pataki et al., 1998], existing CANVEG models poorly reproduce measured CO₂ and H₂O fluxes [Baldocchi, 1997]. In the case of low T_a , current CANVEG models reduce the biochemical kinetic constants and other physiological parameters by a semiempirical temperature response function. It is now recognized that the form of such temperature response functions is sufficiently general but that the coefficients can vary among species [Harley and Baldocchi, 1995]. Hence it is not clear how accurate the temperature response functions must be described in CANVEG models to reproduce CO₂ and H₂O fluxes for low T_a . In the case of low θ , typical leaf-conductance models in CANVEG (e.g., a Ball-Berry-type model) do not consider the reduction in conductance induced by drought effects. It is these hydrologic and climatic conditions that motivated the present study.

Our objective is twofold: (1) to develop stomatal closure corrections that consider the effect of soil moisture deficit on stomatal conductance and to evaluate the performance of the CANVEG model when “generic” biochemical temperature response functions are replaced by species-specific measured functions between the canopy and its microclimate can be collapsed to a single effective layer as in “big-leaf” models. Toward this end, these corrections and formulations are integrated into the Lai et al. [2000] version of the CANVEG model with the aim of evaluating the model performance for a range of hydrologic and climatic conditions.

In particular, we evaluated the revised CANVEG model calculations against eddy-covariance measurements of CO₂ and H₂O fluxes above the canopy. Scaled sap flux measurements are used to estimate bulk canopy conductance for the dominant species in the ecosystem, which in turn, are compared to modeled bulk canopy conductance derived from the CANVEG calculations. A unique feature about the CANVEG approach is its ability to fully resolve the interaction between vegetation and its microclimate, thereby producing realistic solutions that satisfy both the physiological properties and their corresponding microclimate. Hence as an additional line of model evaluations, we will compare predicted and measured mean CO₂ concentration profiles to independently assess the combined source and turbulent dispersion calculations. At its finest scale, the CANVEG model reproduces physiological and biochemical properties of the forest that can be evaluated against measurements made at scales of a whole tree and leaf level with sap flux and porometry. If the model performs well against measurements at ecosystem, tree, and leaf scales, it serves to increase confidence in its ability to correctly describe CO₂ and H₂O exchange processes between the biosphere and the atmosphere. Four experimental periods (each between 7 and 12 days, leading to a total of 1648 half-hour runs) were chosen to contrast periods in which plant stress was caused by drought or low mean air temperatures with predominantly “stress-free” periods.

2. Theory

The CANVEG approach of Baldocchi and Meyers [1998] couples conservation equations for mean scalar mass and heat,

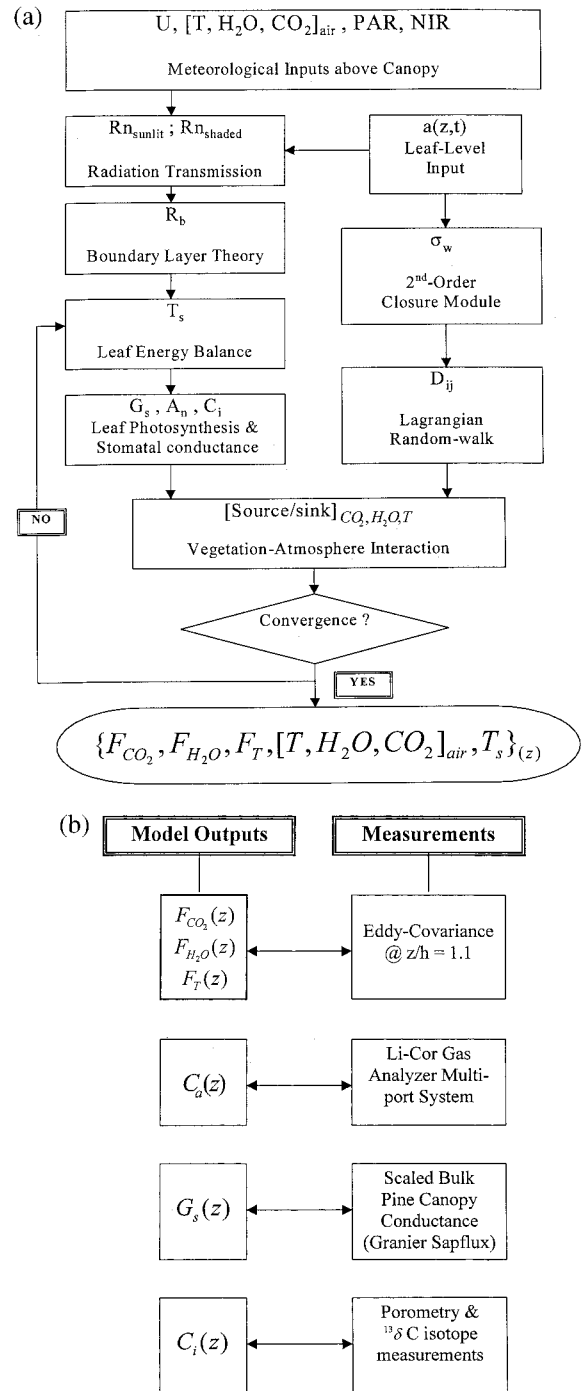


Figure 1. Schematic display of CANVEG framework: (top) Model inputs and operation, (bottom) model outputs and validation.

a Lagrangian turbulent dispersion algorithm, energy and radiation conservation, and biophysical and biochemical mechanisms responsible for stomatal opening and carbon assimilation. Lai et al. [2000] modified the CANVEG approach by using a second-order closure model for momentum and Reynolds stress equations to solve for $\sigma_w(z)$ given a foliage distribution profile. For clarity, we provide a schematic linkage between these conservation equations and submodels as well as the model outputs in Figure 1. In all calculations the canopy height (h) is divided into N layers, each of thickness dz , and all

the schemes listed in Figure 1 are solved iteratively for each discrete layer. Next we provide a brief review of these models.

2.1. Scalar Mass Balance

In a uniform and rigid canopy, the one-dimensional scalar flux budget for a planar homogeneous turbulent flow can be described (after proper time and horizontal averaging) by the scalar conservation equation

$$\frac{\partial \bar{C}}{\partial t} + \frac{\partial F_c}{\partial z} = S_c, \quad (1)$$

where \bar{C} is the mean scalar concentration or temperature (i.e., H₂O, CO₂, and temperature T), F_c is the mean vertical flux of a scalar entity C (e.g., F_{CO_2} , $F_{\text{H}_2\text{O}}$, and F_T are CO₂, H₂O, and sensible heat turbulent fluxes at height z , respectively), and S_c is the mean vegetation source strength at time t and height z above the forest floor. All mean quantities are subject to both time and horizontal averaging as described by *Raupach and Shaw* [1982]. The scalar continuity equation in (1) requires two additional prognostic equations to solve for the three unknowns (\bar{C} , F_c , and S_c).

2.2. Turbulent Dispersion Mechanics

One approach to establish an additional prognostic equation is to consider the interdependency between $S_c(z)$ and $\bar{C}(z)$ via Lagrangian dispersion theory. *Raupach* [1988, 1989] introduced a dispersion matrix (D_{ij}) that relates concentration difference between a given height \bar{C}_z and a reference level above canopy (\bar{C}_r) to the scalar source strength by

$$\bar{C}_z - \bar{C}_r = \sum_{j=1}^N S_{cj} D_{ij} \Delta z_j, \quad (2)$$

where i and j are the indices for concentration and source strength location, respectively, Δz_j is the discrete layer thickness within the canopy, and N is, as before, the number of layers within the canopy volume. The D_{ij} matrix is calculated from the velocity statistics by following the trajectory of an ensemble of fluid parcels released uniformly from a unit source placed at each j th layer. The parcel trajectories and velocities are computed using the random walk algorithm of *Thomson* [1987]. We use the finite difference form of such vertical velocity model in our numerical calculation, as described by *Luhar and Britter* [1989], where

$$w_{i+1} = w_i + \left[-\frac{w_i}{T_L} + \frac{1}{2} \left(1 + \frac{w_i^2}{\sigma_w^2} \right) \frac{\partial \sigma_w^2}{\partial z} \right] \Delta t + \left(\frac{2\sigma_w^2}{T_L} \Delta \right)^{1/2} d\Omega, \quad (3)$$

and w_i is the parcel vertical velocity at time t_i , Δt is the time step increment, and $d\Omega$ is a Gaussian random increment with zero mean and unit variance, and T_L is assumed constant within the canopy as suggested by *Raupach* [1988]. To estimate σ_w and $\partial \sigma_w^2 / \partial z$ in (3), the Eulerian second-order closure model of *Wilson and Shaw* [1977] is adopted. Although third-order closure models have been developed for canopy flows [e.g., *Meyers and Paw U*, 1986; *Meyers and Baldocchi*, 1991], a recent study demonstrated that the model of *Wilson and Shaw* [1977] performs as well as third-order closure models [*Katul and Albertson*, 1998]. The model of *Wilson and Shaw* [1977] assumes steady state adiabatic flow with all triple-velocity

products closed by a gradient-diffusion approximation [*Donaldson*, 1973; *Mellor*, 1973; *Mellor and Yamada*, 1974; *Wilson and Shaw*, 1977; *Shaw*, 1977; *Wilson*, 1988, 1989; *Andren*, 1990; *Canuto et al.*, 1994; *Abdella and McFarlane*, 1997]. The closure model computes vertical variation in mean horizontal velocity, mean momentum flux, and longitudinal, lateral, and vertical velocity standard deviations based on a specified leaf area density and foliage drag coefficient (C_d). The determination of C_d , the specification of boundary conditions, and the numerical implementation of the closure model are described by *Katul and Albertson* [1998] and *Katul and Chang* [1999].

2.3. Physiological Functions

After combining (1) and (2), one additional equation is still required to solve for \bar{C} , F_c , and S_c . This equation is derived from physiological controls on S_c via

$$S_c(z) = -\rho_a a(z) \frac{\bar{C}(z) - \bar{C}_{ic}(z)}{r_b(z) + r_s(z)}, \quad (4)$$

where ρ_a is the mean air density, $a(z)$ is the plant area density, \bar{C}_{ic} is the mean intercellular scalar concentration, $r_b(z)$ is the boundary layer resistance, and $r_s(z)$ is the stomatal resistance. Equations (1), (2), and (4) permit a complete mathematical description of \bar{C} , F_c , and S_c if \bar{C}_{ic} , r_s , and r_b are known or parameterized. The parameterization of these variables is described next.

The estimation of r_b is based on flat plate theory [*Schuepp*, 1993; *Baldocchi and Meyers*, 1998] and is given by

$$r_b = \frac{l_d}{d_m Sh}, \quad (5)$$

where l_d is the characteristic leaf length scale, d_m is the molecular diffusivity of a scalar entity, and Sh is the Sherwood number, which can be determined from the mean longitudinal velocity inside the canopy. While a cylinder flow approximation (vis-à-vis flat plate) is also plausible, the difference between the two formulations of r_b is minor, as demonstrated by *Campbell and Norman* [1998] for Reynolds numbers not exceeding 100,000. Again, the second-order closure model of *Wilson and Shaw* [1977] provides the necessary flow statistics (i.e., mean wind field u) for estimating r_b .

The stomatal conductance G_s ($= r_s^{-1}$) is computed by linking G_s to leaf photosynthesis (A_n), relative humidity (rh), and CO₂ concentration at the leaf surface (C_s), as described by *Ball et al.* [1987] and *Collatz et al.* [1991], and is given by

$$G_s = m \frac{A_n rh}{C_s} + b, \quad (6)$$

where m and b are empirical parameters that vary with vegetation type (but can be independently determined from porometry measurements). The relationship between G_s and A_n in (6) is now widely used in coupling the biochemical model proposed by *Farquhar et al.* [1980] with G_s [*Harley et al.*, 1992; *Baldocchi and Meyers*, 1998]. According to *Farquhar et al.* [1980], A_n is given by

$$A_n \approx \min \left\{ \begin{matrix} J_E \\ J_C \\ J_S \end{matrix} \right\} - R_d, \quad (7)$$

where J_E , J_C , and J_S are the assimilation rates restricted by either electron transport through the photosystem, ribulose

Table 1. Physiological Parameters Used in CANVEG Calculations

| Variable | Value | Unit | Source |
|---|-----------|--------------------------------------|------------------------------------|
| Characteristic leaf length, l_d | 0.001 | m | measurement |
| Spherical leaf distribution, x_e | 1 | | <i>Campbell and Norman</i> [1998] |
| $V_{c \max}$ at 25°C | 59 | $\mu\text{mol m}^{-2} \text{s}^{-1}$ | <i>Ellsworth</i> [1999, 2000] |
| Stomatal slope factor, m | 5.9 (4–9) | | measurement (see Figure 3b) |
| Stomatal intercept factor, b | 0.015 | $\mu\text{mol m}^{-2} \text{s}^{-1}$ | measurement |
| Clumping factor, Π | 0.8 | | <i>Baldocchi and Meyers</i> [1998] |
| Max. quantum efficiency, e_m | 0.08 | | <i>Collatz et al.</i> [1991] |
| Michaelis constant for CO ₂ , K_c | 404 | $\mu\text{mol mol}^{-1}$ | <i>De Pury and Farquhar</i> [1997] |
| Inhibition constant for O ₂ , K_o | 240 | mmol mol^{-1} | <i>De Pury and Farquhar</i> [1997] |
| Leaf absorptivity for PAR, α_p | 0.83 | | measurement |
| CO ₂ /O ₂ specificity ratio, τ | 2.6 | $\text{mmol } \mu\text{mol}^{-1}$ | <i>Collatz et al.</i> [1991] |

bisphosphate carboxylase (or Rubisco), and the export rate of synthesized sucrose, respectively, and R_d is the respiration rate during daytime but in the absence of photorespiration. The details of the formulation and parameterization of J_E , J_C , J_S , and R_d as a function of photosynthetically active radiation (PAR), the intercellular CO₂ concentration (C_i), and surface temperature (T_s) are described in Appendix A. The physiological coefficients used in these calculations are determined from porometry measurements and summarized in Table 1. We note that (6) and (7) require A_n , rh , and T_s within the canopy; hence all three scalars (H₂O, CO₂, and T_a) must be simultaneously considered in (1), (2), and (4) (i.e., nine equations).

2.4. Leaf Energy Balance and Radiative Transfer

An energy budget is employed at the leaf surface for each level within the canopy to compute both mean leaf temperature (T_s) and absorbed radiation. These parameters are necessary to calculate C_i for the $A - C_i$ model of *Farquhar et al.* [1980]. The determination of T_s is critical to modeling photosynthesis because the leaf biochemical reactions inside the chloroplast nonlinearly depend on T_s .

The extraterrestrial radiation was decomposed into solar radiation and thermal radiation. The solar radiation was further divided into direct beam and diffuse radiation [*Campbell and Norman*, 1998]. After subtracting the reflected quantities for PAR and near-infrared radiation (NIR) by the canopy surface, the remaining radiation is transmitted through canopy volume. The light transmission through the canopy is computed for sunlit and shaded portions separately to estimate PAR and NIR irradiance absorbed at each canopy level. This waveband decomposition is necessary because leaf absorptivity is different for these two spectral bands [*Monteith and Unsworth*, 1990; *Campbell and Norman*, 1998]. The light transmission model of *Campbell and Norman* [1998] was used in these calculations and is briefly described below.

The fraction $\tau_b(\psi)$ of incident beam radiation from a zenith angle ψ penetrating the canopy is given by

$$\tau_b(\psi) = \exp(-\sqrt{\alpha} K_{be}(\psi) a_l \Pi), \quad (8)$$

where α is the leaf radiation absorptivity, $K_{be}(\psi)$ is the extinction coefficient for an ellipsoidal leaf distribution [see *Campbell and Norman*, 1998], a_l is the cumulative leaf area density integrated from the canopy top, and Π is the clumping factor of leaf distribution ($\Pi = 1$ when leaves are randomly distributed in space). The model in (8) is sufficiently accurate if $a(z) < 0.5$ for a given layer [*Norman and Welles*, 1983] as is the case for our study.

2.5. Stomatal Closure Induced by Low Temperatures and Droughts

Because assimilation is restricted by T_s [*Björkman et al.*, 1980; *Farquhar et al.*, 1980; *Harley and Tenhunen*, 1991; *Cornic*, 1994], many empirical temperature functions have been proposed to adjust the kinetic coefficients of the *Farquhar et al.* [1980] model [*Johnson and Thornley*, 1985; *Harley et al.*, 1985; *Harley and Tenhunen*, 1991; *Collatz et al.*, 1991; *Campbell and Norman*, 1998]. In our CANVEG framework, explicit accounting for variation in T_s is performed by adjusting the kinetic variables (K_c , K_o , ω , $V_{c \max}$, and R_d ; see Appendix A for definition) using the *Campbell and Norman* [1998] formulation. We also parameterize the same function for temperature corrections to $V_{c \max}$ using porometry $A - C_i$ curve measurements for loblolly pine (*Pinus taeda*) needles collected in February 1999 and August 1999. The $A - C_i$ data consists of measurements of net CO₂ assimilation at light saturation made using a climate-controlled chamber (Li-6400 portable photosynthesis system, Li-Cor) for pine needles that were detached and rehydrated in pure water. Leaf net CO₂ assimilation was measured as a function of C_i for nine different CO₂ levels (ranging from 60 to 1000 $\mu\text{mol CO}_2 \text{ mol}^{-1}$) and three different temperatures (15°, 28°, and 35°C) for three replicate trees at each time of year. Figure 2 shows the comparison of the generic dependence of carboxylation enzyme kinetics $V_{c \max}$ on leaf temperature T_s using the parameterization of *Campbell and Norman* [1998] and the empirical fit of the same function to $A - C_i$ curve porometry measurements for loblolly pines. Our measurements show that for loblolly pine, $V_{c \max}$ increases slightly with T_s , in contrast to the *Campbell and Norman's* [1998] formulation at high temperature. For low temperature conditions, needles in this pine stand remain at about the same $V_{c \max}$ until $T_a < 10^\circ\text{C}$. We assess how sensitive the bulk canopy conductance is to the $V_{c \max}$ parameterization by utilizing both *Campbell and Norman's* and the $V_{c \max} - T_s$ curve derived from $A - C_i$ (Figure 2).

For low soil moisture condition, several investigators heuristically reduced the slope coefficient m in the Ball-Berry model (equation (6)) [*Tenhunen et al.*, 1990; *Williams et al.*, 1996; *Baldocchi*, 1997]. Here we depart from the descriptive approach of *Tenhunen et al.* [1990], water balance approach of *Williams et al.* [1996], or scaling m by a water stress index derived from a precipitation/evaporation ratio [*Baldocchi*, 1997], by proposing a normalized reduction function to modify G_s via soil moisture as

$$G_s = w_r \left[m \frac{A_r rh}{C_s} \right] + b, \quad (9)$$

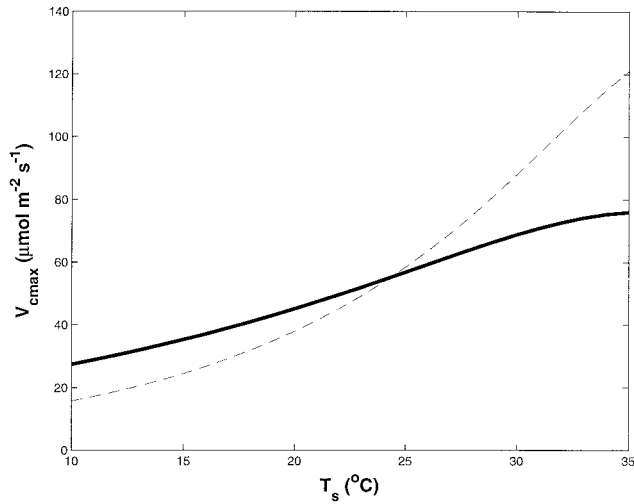


Figure 2. Comparison of the generic dependence of carboxylation enzyme kinetics $V_{c \max}$ on leaf temperature T_s between the parameterization of *Campbell and Norman* [1998] (dashed line) and the empirical fit to $A - C_i$ curve data from loblolly pine measured in both winter and summer months (solid line).

where

$$w_r = \begin{cases} 1 & ; \frac{\bar{\theta}}{\bar{\theta}_R} \geq 1 \\ \frac{f(\bar{\theta})}{f(\bar{\theta}_R)} & ; \frac{\bar{\theta}}{\bar{\theta}_R} < 1 \end{cases} \quad (10a)$$

$$f(\bar{\theta}) = a_m [1 - \exp(-b_m \bar{\theta})] + c_m, \quad (10b)$$

where $\bar{\theta}$ is the mean surface (0–30 cm) soil moisture content, and $\bar{\theta}_R$ is the threshold at which soil moisture content begins to limit stomatal aperture. The determination of $\bar{\theta}_R$ is described in section 3.2.1. The function w_r , applied to every layer in the canopy, is shown in Figure 3a (with $a_m = 83.46$, $b_m = 21.68$, and $c_m = -75.99$) and $f(\bar{\theta})$ is derived from maximum mean canopy stomatal conductance measurements presented by *Oren et al.* [1998a]. Notice in Figure 3a that G_s can decrease by 30% for a $\bar{\theta}$ reduction from 0.2 to 0.15. In (10), when $\bar{\theta} > \bar{\theta}_R$, carbon assimilation and canopy microclimate regulate G_s . However, if $\bar{\theta} < \bar{\theta}_R$, these processes are modulated by hydraulic constraints resulting in nonlinear dependence of m on $\bar{\theta}$.

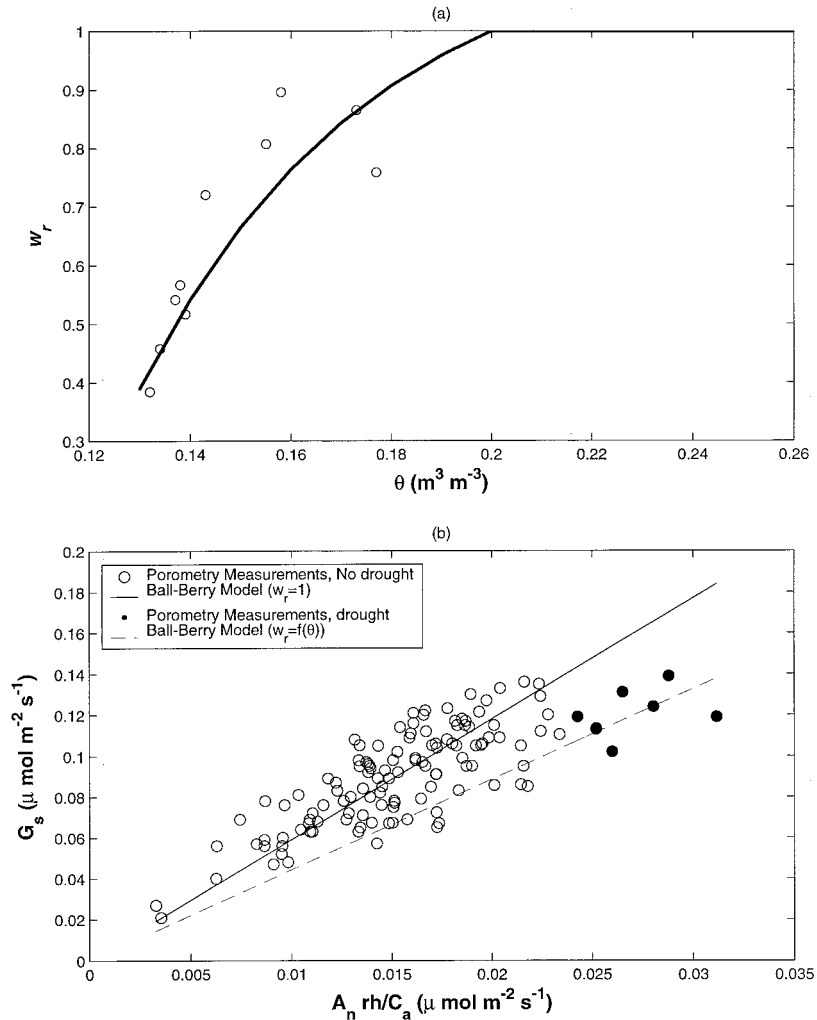


Figure 3. (a) Normalized reduction curve w_r for the slope parameter m in the Ball-Berry stomatal conductance model (solid line). (b) Comparison between G_s from porometry measurements and the Ball-Berry model for drought and nondrought conditions. The open circles represent G_s estimated from daily sap flux measurements reported by *Oren et al.* [1998a].

While w_r in (10) is derived from sap flux measurements, such stomatal decline with decreasing soil moisture content is consistent with the hydraulic limitation approach of *Sperry et al.* [1998]. In their mechanistic approach, hydraulic conductivity in the soil (K_s) and xylem (K_{xylem}) declines with declining water potential (which is related to θ by the soil-water characteristic curve) resulting in a maximum rate of steady state transpiration (E_{crit}) and corresponding minimum leaf water potential at values above which hydraulic failure occurs. Recently, *Ewers et al.* [2000] and *Hacke et al.* [2000] derived the above $w_r - \theta$ relation using this hydraulic limitation approach of *Sperry et al.* [1998] with good agreement reported between model calculations and sap flux measurements. It is not our intent to repeat this derivation or comparison but rather to emphasize that w_r can independently be derived from the hydraulic-cavitation model of *Sperry et al.* [1998].

Our estimate of w_r from sap flux measurements (or hydraulic-cavitation theory) assumes that the same reduction applies at both leaf and canopy scales. In short, (9), (10a), and (10b) assume that w_r is scale independent. We use 3 years of porometry measurements (123 runs) collected for sunlit foliage at the same pine stand [*Ellsworth, 2000*] to further investigate whether signatures of a w_r reduction is present at the leaf scale.

The relationship between measured leaf-level G_s and $A_n rh/C_a$ is presented in Figure 3b for drought (solid circles) and nondrought (open circles) conditions. The slope of this relationship is, by definition, the empirical Ball-Berry m (also shown as solid line), which we determined as 5.9 for nondrought conditions. Clearly, the porometry measurements collected during drought events are lower than this nondrought value. Many nondrought data show m values similar to the identified drought data. These are probably caused by seasonal variation in m , as demonstrated by *Tenhunen et al.* [1990], and will be discussed later. To investigate whether leaf-level measurements experience conductance reduction comparable to the pine canopy scale, the product $w_r m$ was computed from (10a) and (10b) for the drought conditions as a modified slope of the G_s to $A_n rh/C_a$ relationship. It is evident that the revised Ball-Berry model calculations (dashed line, Figure 3b) reproduced the porometry measurements (solid circles) collected during drought conditions better than the mean m . This agreement is consistent with the measured reduction in bulk canopy conductance for low soil moisture content. Such agreement also suggests that the application of (9), (10a), and (10b) with the parameters determined from *Oren et al.* [1998] or the hydraulic-cavitation approach of *Sperry et al.* [1998] is a reasonable approximation of the effect of θ on G_s at the leaf scale in this study site. We compare the computed canopy fluxes with scalar flux measurements above the canopy for both $w_r = 1$ and w_r as a function of the measured θ time series to assess whether the proposed w_r formulation corrects for the effect of drought.

2.6. Model Parameterization, Input, and Output

The model inputs are 30-min mean meteorological conditions at a reference height above the canopy (T_a , H₂O, and CO₂ concentrations, mean longitudinal velocity, and PAR), mean soil moisture content within the root zone, and all radiative, physiological, biochemical, and drag properties of the canopy (particularly $a(z)$, l_d , Π , α , C_d , and the kinetic constants listed in Table 1). All kinetic constants are temperature dependent but assumed to be independent of soil moisture content [*Weber and Gates, 1990; Tenhunen et al., 1990; Sala and*

Tenhunen, 1996; Williams et al., 1996; Baldocchi, 1997], which implies no drought effect on the mesophyll capacity for photosynthesis. The model calculates mean scalar concentrations, sources, and fluxes within and above the canopy for heat, CO₂, and H₂O. Additionally, C_i , T_s , absorbed radiation, and first and second moments of the flow statistics at all levels within the canopy are computed. The lower boundary conditions are soil respiration and evaporation rates. We use the flow statistics from the closure model of *Wilson and Shaw* [1977], and a gradient-diffusion approach just above the forest floor, to estimate the scalar ground fluxes from the mean measured CO₂ and H₂O concentration [see *Lai et al., 2000*] at $z = 0.1$ and 0.75 m. The forest floor is treated as a rough-wall boundary layer in which flux-gradient relationships for CO₂ and H₂O follow similarity theory arguments [*Monin and Yaglom, 1971*].

2.7. Assessment of the Model Performance

The performance of the CANVEG model, modified to incorporate the effects of soil moisture deficit and low air temperature, is assessed by comparing predicted CO₂ and H₂O fluxes above the canopy against eddy-covariance F_{CO_2} and $F_{\text{H}_2\text{O}}$ measurements, and sap flux scaled stand transpiration (E_c). The calculations of radiation/energy balance are indirectly evaluated by comparing predicted and eddy-covariance measured F_T above the canopy. Additionally, at the canopy scale, the modeled CO₂ concentration inside the canopy is compared with measured mean CO₂ concentration to assess the adequacy of the source/dispersion calculations.

At a finer scale, the model is assessed for its ability to reproduce the essential biophysical and biochemical controls on CO₂ and H₂O sources and fluxes. This is done by comparing the bulk canopy conductance (G_m) derived from the modeled $r_s(z)$ for pine foliage only with the scaled conductance (G_c) estimated from E_c measurements collected within pine trees. For the scaled canopy conductance comparisons, we choose the sap flux measurements as our reference because they are not influenced by soil evaporation, and they uniquely define the pine transpiration and bulk conductance. This latter point is critical because the CANVEG model assumes uniform pine physiology over the entire leaf area while eddy-covariance measurements are influenced by nonpine understory flux contribution. Sap flux measurements isolate the flux contribution of the pine trees in the stand from the ecosystem flux and hence are better suited to assess the overall CANVEG conductance calculations.

As a final line of testing the model, we used C_i/C_a estimates representing long-term average from ¹³δC isotope analysis [*Ellsworth, 1999*] and instantaneous values from leaf-level gas exchange measurements to evaluate whether the model reasonably reproduces the biochemical mechanisms of CO₂ assimilation. The measurements used to evaluate the model outputs are shown in Figure 1.

3. Experiment

3.1. Study Site

Measurements were made at the Blackwood Division of the Duke Forest near Durham, North Carolina (36°2'N, 79°8'W, elevation = 163 m). The site is a uniformly planted loblolly pine (*Pinus taeda* L.) forest that extends 300–600 m in the east-west direction and 1000 m in the north-south direction. The mean canopy height (h) was 14 m (± 0.5 m) at the time of the experiment. The topographic variations are small (terrain

Table 2. Plant Area Index (PAI) and Hydrological and Environmental Conditions for Four Study Periods

| Period | PAI | P_r , mm | T_a , °C | | $\bar{\theta}$, cm ³ cm ⁻³ | | R_n , ^b W m ⁻² | | |
|--|-----|------------------------|------------|------|---|------|--|-------|-------|
| | | | Mean | s.d. | Mean | s.d. | Mean | Max | |
| 07/16/98 / 07/28/98 04/02/99 / 04/11/99 11/17/98 / 11/24/98 01/26/99 / 01/31/99 | 1 | 2.69/4.89 ^a | 0 | 27.4 | 4.0 | 0.15 | 0.002 | 429.2 | 745.8 |
| | 2 | 2.02 | 35.2 | 18.6 | 5.2 | 0.36 | 0.02 | 332.2 | 710.0 |
| | 3 | 2.89 | 3.9 | 11.7 | 5.7 | 0.30 | 0.01 | 115.9 | 345.6 |
| | 4 | 2.00 | 0 | 9.5 | 5.7 | 0.24 | 0.01 | 212.8 | 471.8 |

s.d., standard deviation; max, maximum.

^aPAI for the whole stand, including pine and understory foliage; other PAIs are for pine component of the stand only.

^bDaytime (0900–1500) average.

slope changes <5%) so that the influence of topography on the turbulence transport can be neglected [Kaimal and Finnigan, 1994].

3.2. Measurement Periods

Four experimental periods (each between 7 and 12 days) were chosen to investigate potential plant stress due to drought and low mean air temperature. These periods were in July 1998, November 1998, January 1999, and April 1999 and are described below.

3.2.1. Drought period. In July 1998 the measured precipitation was well below the long-term average for the month. We computed the long-term mean precipitation ($= 121.4 \pm 60.5$ mm) for July by averaging 67 years of monthly precipitation collected from a nearby weather station. The measured monthly precipitation in July 1998 was 24.4 mm, which is less than 30% of the long-term average. At this site, more than 90% of the water uptake by pine roots occurs in the top 30-cm soil layer [Oren *et al.*, 1998a]. Thus drought effects are related to the near-surface (30 cm) horizontally averaged volumetric soil moisture content ($\bar{\theta}$), which was shown to exert a strong control over canopy stomatal conductance for $\bar{\theta} < 0.2$ ($= \bar{\theta}_R$). The time variation of $\bar{\theta}$ was measured by averaging 24 30-cm vertical reflectometer rods (CS615, Campbell Scientific, Logan, Utah) distributed throughout the study site.

The $\bar{\theta}$ measurements in July 1998 confirmed that the low precipitation resulted in soil drought ($\bar{\theta} \cong 0.15$ cm³ cm⁻³, $< \bar{\theta}_R$). To investigate the effect of drought on CO₂ and H₂O fluxes, we selected a 12-day experimental duration (period 1, July 16–28, 1998) in which eddy-covariance F_{CO_2} and F_{H_2O} , sap flux, and θ measurements were simultaneously available with few interruptions and gaps within the record. A “reference” period for assessing the performance of the CANVEG model under well-watered condition was also selected. This period (period 2, April 2–11, 1999) was characterized by $\bar{\theta} > 0.27$ over the entire duration (i.e., $\bar{\theta} > \bar{\theta}_R$).

3.2.2. Low air temperature. The reduction in CO₂ assimilation and transpiration rate caused by low mean air temperature was investigated using two periods (period 3, November 17–24, 1998, and period 4; January 26–31, 1999). The mean T_a for these two periods were $11.7 \pm 5.7^\circ\text{C}$ and $9.5 \pm 5.7^\circ\text{C}$, respectively. Stomata of loblolly pine close in response to low

temperature when $T_a < 10^\circ\text{C}$ [Ellsworth, 2000]. On the basis of these findings, period 3 represents mild winter conditions when stomata should not appreciably respond to low T_a , while during period 4, low T_a should reduce stomatal conductance and exchanges of H₂O and CO₂. We note that both soil moisture and temperature regulation are unlikely to be threshold phenomena, so while periods are selected in which the current data would suggest strong regulation by these factors, there may be interactions between $\bar{\theta}$ and T_a and other environmental factors not explicitly considered here. Table 2 summarizes the climatic and hydrologic conditions along with the measured plant area index (PAI) for these four experimental periods.

3.3. Eddy Covariance Measurements

The F_{CO_2} , F_{H_2O} , and F_T turbulent fluxes were measured by an eddy-covariance system composed of a CO₂/H₂O infrared gas analyzer (Licor-6262, LI-COR, Lincoln, Nebraska), a tri-axial sonic anemometer (CSAT3, Campbell Scientific, Logan, Utah), and a krypton hygrometer (KH₂O, Campbell Scientific). The anemometer and hygrometer were positioned 15 m above the ground surface and anchored on a horizontal bar extending 1.5 m away from the walk-up tower. The hygrometer was used to assess and correct tube attenuation effects and lagged maximum cross correlation between the vertical velocity and the measured scalar concentration as discussed by Katul *et al.* [1997a, 1997b]. Analog signals from these instruments were sampled at 10 Hz using a Campbell Scientific 21X data logger. All the digitized signals were transferred to a portable computer via an optically isolated RS232 interface for future processing. Raw 10 Hz measurements were processed using the procedures described by Katul *et al.* [1997a, 1997b].

It must be emphasized that these flux measurements were conducted in the canopy sublayer but not the atmospheric surface layer; hence the spatial variability in scalar fluxes is larger due to the influence of “near-field” source variability. In fact, a recent spatial variability experiment, conducted at this site, suggests that the scalar fluxes near the canopy-atmosphere interface vary by about 20% [Katul *et al.*, 1999]. Hence for practical purposes, we use the term “close agreement” when the CANVEG model reproduces the measured fluxes to within 20%. This estimate is consistent with a recent estimate by Moncrieff *et al.* [1996] which also showed eddy-covariance mea-

measurements possess $\pm 20\%$ combined random and systematic errors.

3.4. Other Meteorological Variables

In addition to the flux measurements, a Ta/RH probe (HMP35C, Campbell Scientific) was positioned at 15.5 m to measure the mean T_a and relative humidity. A Fritchen-type net radiometer and a quantum sensor (Q7 and LI-190SA, respectively, LI-COR) were installed to measure net radiation (R_n) and PAR, respectively. All the meteorological variables were sampled at 1 s and averaged every 30 min using a 21X Campbell Scientific data logger.

3.5. CO₂/H₂O Profiles Within the Canopy

A multiport system was installed to measure the CO₂/H₂O concentrations inside the canopy at 10 levels (0.1, 0.75, 1.5, 3.5, 5.5, 7.5, 9.5, 11.5, 13.5, and 15.5 m). Each level was sampled for 1 min (45 s sampling and 15 s purging) at the beginning, the middle, and the end for each 30-min sampling period. The flow rate within the tube (internal diameter = 0.423 cm) was 0.9 L min⁻¹ to dampen all turbulent fluctuations.

3.6. Xylem Sap Fluxes

Sap flow (in g H₂O m⁻² sapwood s⁻¹) within eight individual pine trees was measured with constant-heat probes [Granier, 1987]. Sap flux densities of individual trees were scaled to attain a plot-level values using the respective sapwood area per unit ground area in the stand [Phillips and Oren, 1998; Oren et al., 1998b].

3.7. Leaf-Level Physiological Parameters

The leaf-level measurements presented in Table 1 are described by Ellsworth [1999, 2000] and are briefly repeated here for completeness. The leaf-level physiological parameters (m and b) were determined from gas exchange measurements (see Figure 3b) by a portable infrared gas analyzer system for CO₂ and H₂O (CIRAS-1, PP-Systems) operated in open flow mode with a 5.5-cm-long leaf chamber and an integrated CO₂ gas supply system. The chamber was modified with an attached Peltier cooling system to maintain chamber temperature near ambient atmospheric temperature. The data were collected for upper canopy foliage at 11–12 m height, accessed with a system of towers and mobile, vertically telescoping lifts. All measured gas exchange rates reported here are on a unit-projected area basis. These measurements were collected over a broad range of environmental and hydrologic conditions spanning a period of nearly 3 years (May 1997 to March 2000).

3.8. Leaf Area Density

The vertical variation of the leaf area plus branches was measured by gap fraction techniques following theory presented by Norman and Welles [1983]. A pair of optical sensors with hemispherical lenses (LAI-2000, Li-Cor, Lincoln, Nebraska) was used for canopy light transmittance measurements from which gap fraction and plant area densities were calculated. The measurements were made at 1-m intervals from the top of the canopy to 1 m above the ground to produce the vertical profile in plant area index (PAI). PAI measurements were made within 2 weeks of each of the measurement periods, from the same tower used for measuring flow statistics, CO₂ concentration, and F_{CO_2} and F_{H_2O} .

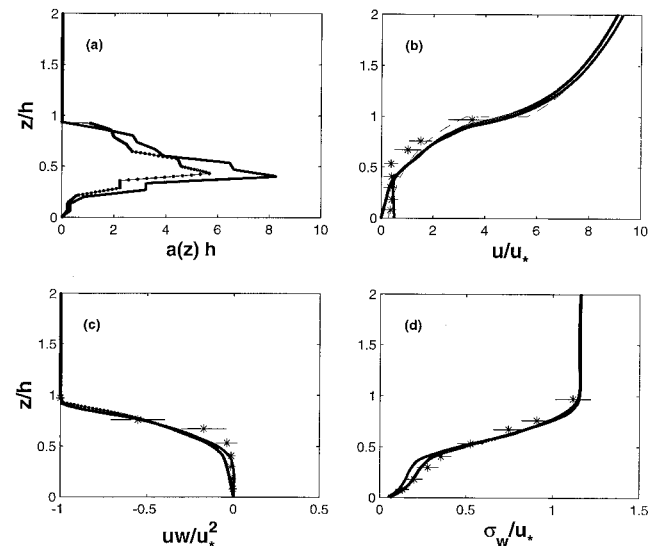


Figure 4. Effect of leaf area density dynamics on modeled velocity statistics. Modeled flow statistics inside the canopy are conducted for two different plant area index (PAI) values, one collected during the summer (maximum PAI) and the other collected during winter (minimum PAI) are discussed. The modeled statistics for maximum and minimum PAI are shown in solid line and open circle line, respectively. Triaxial sonic anemometry measurements (star) collected in August 1999 are also shown for reference. (a) Maximum and minimum measured plant area density $a(z)$. (b) Comparison between modeled \bar{u} using the commonly assumed exponential profiles inside the canopy (dashed line), and the closure model calculations for the two PAI profiles in Figure 4a. (c) The maximum effect of variable PAI on modeled \overline{uw} . (d) The maximum effect of variable PAI on modeled σ_w .

4. Results and Discussion

4.1. Flow Statistics

Before investigating the scalar transport, we briefly describe the flow statistics within the canopy. Figure 4 shows the velocity statistics inside the canopy predicted by the second-order closure model [Wilson and Shaw, 1977], based on the measured plant area density for two cases: highest foliage density in July and lowest in January. To demonstrate the differences in the flow statistics resulting from these two PAI extremes, we compared the mean longitudinal wind velocity (\bar{u}), shear stress (\overline{uw}), and standard deviation of vertical velocity (σ_w) for the two plant area density profiles ($a(z)$). In this comparison the velocity scales are normalized by u_* at $z/h = 1.1$ and the length scales are normalized by h . As shown in Figure 4, the modeled flow statistics (particularly σ_w) are fairly robust to variations in plant area density. However, the $d\sigma_w/dz$, which is crucial to the Lagrangian random walk calculation as in (3), is sensitive to variations in PAI. Such variations in $d\sigma_w/dz$ can affect D_{ij} and the scalar concentration as demonstrated by the detailed sensitivity analysis of Lai et al. [2000].

4.2. Comparisons of CO₂ and H₂O Fluxes

To compute $F_{CO_2}(h)$, $F_{H_2O}(h)$, and $F_T(h)$, steady state conditions are first assumed. Over tall forests such an approximation may produce a bias if the CO₂ storage flux is significant [Wofsy et al., 1993; Hollinger et al., 1994; Fan et al., 1995; Grace et al., 1995; Baldocchi et al., 1997; Lee, 1998]. Earlier estimates

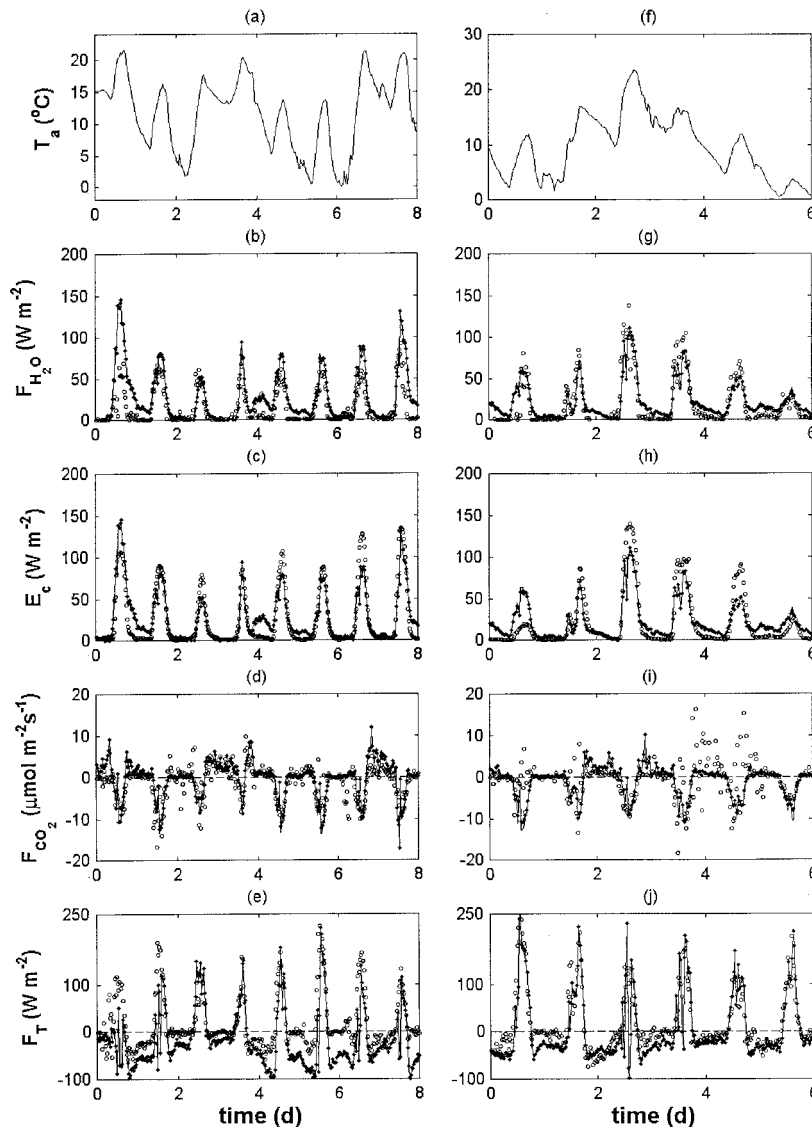


Figure 5. Effect of different $V_{c \max} - T_s$ formulations shown in Figure 2 on CANVEG-modeled $F_{\text{H}_2\text{O}}$, F_{CO_2} , and F_T for moderately low temperature period 3 (left column) and low temperature period 4 (right column). Solid line is the CANVEG fluxes using the pine-specific $V_{c \max} - T_s$, dots represent the CANVEG fluxes using the generic form of $V_{c \max} - T_s$ [Campbell and Norman, 1998], and open circles are for eddy-covariance or sap flux (E_c) measurements. The eddy-covariance measurements were conducted at $z/h = 1.1$.

of mean CO₂ concentration from measurements within this stand demonstrated that the CO₂ storage flux is much smaller than the CO₂ flux above the canopy, except in early morning and late afternoon hours [Lai et al., 2000]. Therefore the CO₂ storage flux is assumed negligible relative to $F_{\text{CO}_2}(h)$ in all four periods.

4.2.1. Temperature effects on fluxes. To evaluate the dependency of the kinetic constants on temperature as in the work of Campbell and Norman [1998] (Appendix A), we compared the modeled $F_{\text{CO}_2}(h)$ and $F_{\text{H}_2\text{O}}(h)$ with eddy-covariance measurements using the two $V_{c \max} - T_s$ relationships shown in Figure 2. For period 3 (the “stress-free” period) the model estimates closely follow the measured diurnal patterns of $F_{\text{CO}_2}(h)$ and $F_{\text{H}_2\text{O}}(h)$ for both $V_{c \max} - T_s$ functions (Figure 5). To verify the model performance using another independent measure, we also show the sap flux scaled E_c time

series in Figures 5c and 5h. While the regression statistics in Table 3 suggest some biases between measured and modeled fluxes (see regression slopes), the root-mean-square errors are relatively small ($<30 \text{ W m}^{-2}$ for water vapor). The reason for such a bias will be discussed later in the sensitivity analysis. Regardless of the bias, it is important to note that the difference between the resulting H₂O and the CO₂ fluxes is small when either $V_{c \max} - T_s$ relationship is used, suggesting that the CANVEG flux calculations are not very sensitive to the $V_{c \max}$ formulation.

4.2.2. Soil moisture effects on fluxes. During the drought (period 1), soil moisture content was well below $\bar{\theta}_R (= 0.2)$, the threshold below which $\bar{\theta}$ begins to exert control over stomata, while during the reference period (period 2), $\bar{\theta}$ was consistently $>\bar{\theta}_R$ (see Figures 6a and 6f). The modeled $F_{\text{H}_2\text{O}}(h)$, $F_{\text{CO}_2}(h)$, and $F_T(h)$ are compared with the eddy-

Table 3. Regression Statistics for Comparisons Between Measurement and Model Estimation

| Variable | Measurement/Model Type | N_r | A | B | R^2 | RMSE |
|--|-----------------------------------|-------|------|--------|-------|-------|
| Period 1, July 1998 | | | | | | |
| $[F_{\text{H}_2\text{O}} (\text{W m}^{-2})]$ | eddy covariance at $z/h = 1.1$ | 544 | 0.99 | -10.68 | 0.83 | 35.05 |
| $F_{\text{H}_2\text{O}} (\text{W m}^{-2})$ | eddy covariance at $z/h = 1.1$ | 544 | 0.84 | -6.78 | 0.86 | 38.17 |
| $[F_{\text{H}_2\text{O}} (\text{W m}^{-2})]$ | xylem sap flux | 544 | 0.91 | -3.85 | 0.94 | 15.47 |
| $F_{\text{H}_2\text{O}} (\text{W m}^{-2})$ | xylem sap flux | 544 | 0.75 | -1.47 | 0.95 | 24.28 |
| $[F_{\text{CO}_2} (\mu\text{mol m}^{-2} \text{s}^{-1})]$ | eddy covariance at $z/h = 1.1$ | 544 | 1.09 | -1.59 | 0.53 | 6.17 |
| $F_{\text{CO}_2} (\mu\text{mol m}^{-2} \text{s}^{-1})$ | eddy covariance at $z/h = 1.1$ | 544 | 1.02 | -1.40 | 0.54 | 0.49 |
| $[F_T (\text{W m}^{-2})]$ | eddy covariance at $z/h = 1.1$ | 544 | 0.73 | 45.86 | 0.83 | 73.12 |
| $F_T (\text{W m}^{-2})$ | eddy covariance at $z/h = 1.1$ | 544 | 0.95 | 59.26 | 0.75 | 73.12 |
| $[G_m/G_c (\text{mm s}^{-1})]$ | loblolly pine measurement | 478 | 0.84 | -0.22 | 0.79 | 0.64 |
| $G_m/G_c (\text{mm s}^{-1})$ | loblolly pine measurement | 478 | 0.58 | -0.008 | 0.79 | 1.03 |
| Period 2, April 1999 | | | | | | |
| $F_{\text{H}_2\text{O}} (\text{W m}^{-2})$ | eddy covariance at $z/h = 1.1$ | 421 | 1.20 | -2.26 | 0.86 | 29.36 |
| $F_{\text{H}_2\text{O}} (\text{W m}^{-2})$ | xylem sap flux | 421 | 0.87 | 2.25 | 0.76 | 29.39 |
| $F_{\text{CO}_2} (\mu\text{mol m}^{-2} \text{s}^{-1})$ | eddy covariance at $z/h = 1.1$ | 421 | 0.85 | -0.16 | 0.56 | 4.64 |
| $F_T (\text{W m}^{-2})$ | eddy covariance at $z/h = 1.1$ | 421 | 0.80 | -3.92 | 0.87 | 40.48 |
| $G_m/G_c (\text{mm s}^{-1})$ | loblolly pine measurement | 242 | 0.81 | 0.25 | 0.70 | 1.19 |
| Period 3 ^a , Nov. 1998 | | | | | | |
| $F_{\text{H}_2\text{O}} (\text{W m}^{-2})$ | eddy covariance at $z/h = 1.1$ | 384 | 0.55 | -1.09 | 0.61 | 23.78 |
| $F_{\text{H}_2\text{O}} (\text{W m}^{-2})$ | xylem sap flux | 384 | 1.05 | -2.45 | 0.83 | 14.98 |
| $F_{\text{CO}_2} (\mu\text{mol m}^{-2} \text{s}^{-1})$ | eddy covariance at $z/h = 1.1$ | 384 | 0.60 | -0.95 | 0.50 | 3.35 |
| $F_T (\text{W m}^{-2})$ | eddy covariance at $z/h = 1.1$ | 384 | 0.71 | 30.25 | 0.52 | 56.85 |
| $G_m/G_c (\text{mm s}^{-1})$ | loblolly pine measurement | 132 | 1.22 | -0.65 | 0.71 | 1.04 |
| Period 4 ^b , Jan. 1999 | | | | | | |
| $F_{\text{H}_2\text{O}} (\text{W m}^{-2})$ | eddy covariance at $z/h = 1.1$ | 288 | 1.09 | -6.79 | 0.75 | 15.42 |
| $F_{\text{H}_2\text{O}} (\text{W m}^{-2})$ | xylem sap flux | 288 | 1.29 | -7.63 | 0.79 | 16.88 |
| $F_{\text{CO}_2} (\mu\text{mol m}^{-2} \text{s}^{-1})$ | eddy covariance at $z/h = 1.1$ | 288 | 0.48 | -0.11 | 0.20 | 4.37 |
| $F_T (\text{W m}^{-2})$ | eddy covariance at $z/h = 1.1$ | 288 | 0.79 | 13.85 | 0.69 | 41.63 |
| $G_m/G_c (\text{mm s}^{-1})$ | loblolly pine measurement | 56 | 0.83 | 1.84 | 0.52 | 1.60 |
| $G_m/G_c (\text{mm s}^{-1})$ | <i>Campbell and Norman</i> [1998] | 56 | 0.85 | 1.81 | 0.51 | 1.63 |
| Other variables | | | | | | |
| C_a^b , ppm | gas analyzer at 6 levels | 9822 | 1.07 | -26.50 | 0.87 | 10.53 |
| $F_{\text{CO}_2} (\mu\text{mol m}^{-2} \text{s}^{-1})$ | big-leaf model (period 2) | 421 | 0.68 | 2.14 | 0.54 | 6.66 |
| $F_{\text{CO}_2} (\mu\text{mol m}^{-2} \text{s}^{-1})$ | big-leaf model (period 3) | 384 | 0.46 | 1.19 | 0.48 | 5.77 |
| $F_{\text{CO}_2} (\mu\text{mol m}^{-2} \text{s}^{-1})$ | big leaf/CANVEG (period 2) | 421 | 0.89 | 2.75 | 0.94 | 3.88 |
| $F_{\text{CO}_2} (\mu\text{mol m}^{-2} \text{s}^{-1})$ | big leaf/CANVEG (period 3) | 384 | 0.71 | 3.27 | 0.83 | 5.38 |
| D/D_a (kPa) | CANVEG model | 1415 | 0.96 | 0.05 | 0.99 | 0.08 |

The regression slope (A), the intercept (B), the coefficient of determination (R^2), and the root-mean-square error (RMSE) are presented for the regression model $y = Ax + B$, where y and x are measured and modeled variables, respectively. Modeled H₂O fluxes are compared with measurements conducted by eddy-covariance and sap-flux techniques. G_c and G_m are the bulk canopy conductance computed by equations (11) and (13), respectively. C_a is the mean CO₂ concentration inside the canopy and N_r is the number of points in the regression analysis. For G_m/G_c comparison, x is G_m . For period 1, variables in brackets are regression results after implementing soil moisture correction for the drought effect in the modeled G_s . For period 4, G_m/G_c comparison was shown for the temperature dependency of $V_{c \max}$ derived from *Campbell and Norman* [1998] and measurement performed on the loblolly pine. For the comparison between big-leaf and CANVEG models, x is the value of big-leaf calculation.

^aComparisons are for the measured $V_{c \max} - T_s$ relationship of Figure 2. Similar statistics were found for the *Campbell and Norman* [1998] formulation and hence are not displayed.

^bCombined regression statistics are shown for all four periods and the six selected levels.

covariance measurements for these two periods in Figure 6. When $\bar{\theta} > \bar{\theta}_R$, modeled fluxes are close to measured fluxes (see Figures 6g, 6h, and 6i), consistent with findings in other studies [Amthor et al., 1994; Baldocchi and Harley, 1995; Leuning et al., 1995; Aber et al., 1996; Williams et al., 1996; Baldocchi and Meyers, 1998; Gu et al., 1999]. When $\bar{\theta} < \bar{\theta}_R$, the modeled H₂O fluxes departed from the measured fluxes when w_r was not applied in CANVEG calculation (see regression slopes in Table 3). These calculations overestimated measured $F_{\text{H}_2\text{O}}(h)$ by 16%. With the w_r modification the CANVEG overestimated measured $F_{\text{H}_2\text{O}}(h)$ by only 1% (see regression slope in Table 3) which is not significantly different from unity ($P > 0.05$). However, we found that the w_r improvements in modeling $F_{\text{H}_2\text{O}}(h)$ degraded the comparison with the measured $F_{\text{CO}_2}(h)$ ($P < 0.05$, Table 3). We attribute the effect of the w_r correction to the significant proportion of understory foliage (45% of total PAI) during the summer period, which contributes more to $F_{\text{CO}_2}(h)$ than to $F_{\text{H}_2\text{O}}(h)$. We evaluated

this hypothesis by repeating the CANVEG calculation on the pine foliage only with and without the w_r adjustment and comparing these two calculations with the E_c estimated from sap flux measurements (Figures 6c and 6h). Consistent with eddy-covariance comparisons, the w_r correction resulted in better agreement between E_c and modeled pine latent heat flux, suggesting that the CANVEG model correctly reduced the pine transpiration for drought conditions. Because pine transpiration, unlike pine photosynthesis, comprises most of the total mass flux (e.g., $F_{\text{H}_2\text{O}}(h)$), the w_r correction was important in improving the model agreement with eddy-covariance-measured $F_{\text{H}_2\text{O}}(h)$. We hypothesize that the understory species contribute relatively more to total stand $F_{\text{CO}_2}(h)$ than to $F_{\text{H}_2\text{O}}(h)$ under drought conditions. We explore this hypothesis using detailed sensitivity analysis discussed next.

4.2.3. Sensitivity analysis on fluxes. The inconsistency in model performance led us to conduct a detailed sensitivity

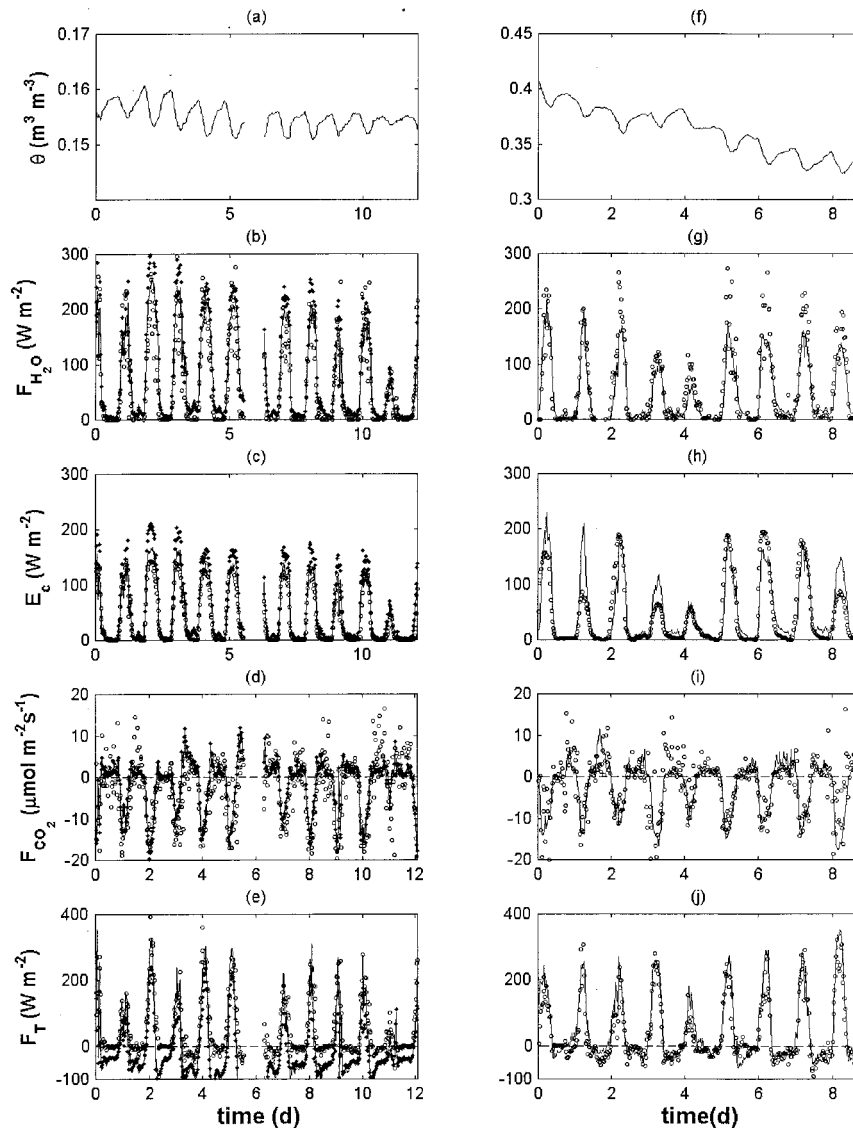


Figure 6. Effect of drought on CANVEG modeled $F_{\text{H}_2\text{O}}$, F_{CO_2} , and F_T for the drought period 1 (left column) and the stress-free period 2 (right column). Solid line is the CANVEG fluxes using $w_r \neq 1$, dots represent CANVEG fluxes for $w_r = 1$, and open circles are for eddy-covariance or sap flux (E_c) measurements. For the E_c comparisons (Figures 6c and 6h), the PAI for pine only is used in the CANVEG calculations. A short (<1 day) data gap exists in period 1. For period 2, $w_r = 1$ is used throughout. The eddy-covariance measurements were conducted at $z/h = 1.1$.

analysis on how modeled water vapor and CO₂ flux errors vary with m for all four periods. We varied m from 3.0 to 9.0 and computed the root-mean-square error (RMSE) and the regression slope of fluxes measured with eddy covariance versus modeled fluxes (Table 4). These two statistics were chosen to assess the magnitude of the scatter (RMSE) and model bias (the regression slope). We found that modeled $F_{\text{H}_2\text{O}}(h)$ (without any w_r adjustments) is much more sensitive to variations in m than $F_{\text{CO}_2}(h)$ except in period 1, the drought period. In all other periods the RMSE and regression slopes appear robust to variations in m for $F_{\text{CO}_2}(h)$ estimates. This is not surprising given that many factors influence $F_{\text{CO}_2}(h)$ (such as soil respiration); however, variations in $F_{\text{H}_2\text{O}}(h)$ are intimately linked with G_s , thereby increasing their sensitivity to m .

In the drought period (period 1), m optimized by water vapor was reduced by about 30% when compared to its well-

watered state, consistent with the w_r reduction derived from Figure 3. However, m optimized by CO₂ for period 1 is 1.6 times larger than its counterpart for $F_{\text{H}_2\text{O}}(h)$, suggesting that an effective m (and subsequent drought reductions) solely derived from pine physiological measurements does not represent the entire ecosystem $F_{\text{CO}_2}(h)$ during summer droughts. Consequently, we conclude that the understory physiological attributes and their separate response to drought must be considered when estimating $F_{\text{CO}_2}(h)$.

An interesting finding from Table 4 is that the optimum m required to minimize the RMSE and recover a unit regression slope varied among periods for $F_{\text{H}_2\text{O}}(h)$. Whether the variations in m among periods is an artifact of the sensitivity, measurement errors, or a real physiological signature requires further investigation. Using the 3-year porometry record shown in Figure 3b, we estimated the leaf-level m for each porometry

Table 4. Sensitivity Analysis of CO₂ and Water Vapor Fluxes Above the Canopy on the Ball-Berry Stomatal Conductance Parameter m

| m | Period 1 | | Period 2 | | Period 3 | | Period 4 | |
|-------|------------------|-----------------|------------------|-----------------|------------------|-----------------|------------------|-----------------|
| | H ₂ O | CO ₂ | H ₂ O | CO ₂ | H ₂ O | CO ₂ | H ₂ O | CO ₂ |
| RMSE | | | | | | | | |
| 3.0 | 37.46 | 6.31 | | | (20.09) | (3.27) | 17.72 | (4.29) |
| 3.5 | 36.09 | 6.25 | | | 20.51 | 3.30 | 17.10 | 4.31 |
| 4.0 | 35.26 | 6.19 | 32.77 | (4.70) | 21.03 | 3.31 | 16.56 | 4.32 |
| 4.5 | (35.06) | 6.14 | 30.10 | 4.71 | 21.65 | 3.32 | 16.12 | 4.34 |
| 5.0 | 35.54 | 6.10 | 27.96 | 4.79 | 22.34 | 3.34 | 15.77 | 4.35 |
| 5.5 | 36.73 | 6.06 | 26.48 | 4.85 | 23.11 | 3.33 | 15.53 | 4.36 |
| 6.0 | 38.60 | 6.03 | (25.80) | 4.87 | 23.95 | 3.34 | 15.41 | 4.37 |
| 6.5 | 41.06 | 6.01 | 26.00 | 4.87 | 24.85 | 3.35 | (15.40) | 4.37 |
| 7.0 | 44.04 | 5.99 | 27.04 | 4.91 | 25.80 | 3.36 | 15.50 | 4.38 |
| 7.5 | 47.46 | (5.97) | 28.83 | 4.97 | 26.79 | 3.36 | 15.72 | 4.39 |
| 8.0 | | | 31.24 | 4.99 | 27.82 | 3.36 | 16.04 | 4.39 |
| 8.5 | | | 34.14 | 5.01 | 28.90 | 3.37 | 16.46 | 4.40 |
| 9.0 | | | 37.39 | 5.06 | 30.00 | 3.36 | 16.97 | 4.40 |
| Slope | | | | | | | | |
| A | | | | | | | | |
| 3.0 | 1.08 | 1.16 | | | (0.65) | (0.63) | 1.47 | (0.50) |
| 3.5 | 1.04 | 1.13 | | | 0.63 | 0.62 | 1.40 | 0.50 |
| 4.0 | (1.00) | 1.10 | 1.31 | (0.81) | 0.61 | 0.61 | 1.33 | 0.49 |
| 4.5 | 0.96 | 1.08 | 1.23 | 0.80 | 0.59 | 0.61 | 1.26 | 0.49 |
| 5.0 | 0.91 | 1.05 | 1.15 | 0.78 | 0.58 | 0.60 | 1.20 | 0.49 |
| 5.5 | 0.87 | 1.03 | 1.08 | 0.77 | 0.56 | 0.60 | 1.14 | 0.48 |
| 6.0 | 0.83 | 1.02 | (1.01) | 0.76 | 0.54 | 0.60 | 1.08 | 0.48 |
| 6.5 | 0.80 | (1.00) | 0.95 | 0.75 | 0.53 | 0.60 | 1.04 | 0.48 |
| 7.0 | 0.76 | 0.98 | 0.90 | 0.75 | 0.51 | 0.60 | (0.99) | 0.48 |
| 7.5 | 0.73 | 0.97 | 0.86 | 0.74 | 0.50 | 0.60 | 0.95 | 0.48 |
| 8.0 | | | 0.81 | 0.73 | 0.48 | 0.60 | 0.91 | 0.48 |
| 8.5 | | | 0.77 | 0.73 | 0.47 | 0.59 | 0.87 | 0.47 |
| 9.0 | | | 0.74 | 0.72 | 0.45 | 0.59 | 0.84 | 0.47 |

Both root-mean-square error (RMSE) and regression slope A of the regression model $y = Ax + B$ (y = measured flux, x = CANVEG modeled flux) are shown. Numbers in parentheses indicate optimum values.

measurement. These m values are shown as a function of time (Figure 7a) to investigate potential seasonal variations in leaf physiological properties as reported by *Tenhunen et al.* [1990]. It is clear that the scatter in leaf-level m is large, but the signature of a seasonal pattern is discernible. When combined with the sensitivity analysis of Table 4, Figure 7a suggests that m is lowest in the middle of the growing season, with a rise later in the season concurrent with maturation of new pine needles. In fact, the trends in the optimized m are consistent with the leaf-level ensemble-averaged m (Figure 7b). Thus it is not surprising that the CANVEG model, with static vegetation parameters such as m (= 5.9), shows inconsistent performance among periods. We also point out that seasonal variations in leaf-level m (Figure 7a) are larger than the maximum drought correction encountered in this experiment, suggesting that using CANVEG for estimating annual carbon uptake requires estimates of the seasonal variability in its physiological parameters (e.g., m).

4.3. Comparisons of Sensible Heat Flux

An indirect assessment of the radiation transmission and energy distribution of the CANVEG model is performed by comparing the modeled $F_T(h)$ with values from eddy-covariance measurements shown in Figures 5 and 6 for all four periods. Despite the underestimation in period 3, and some discrepancy during evening runs, the daytime diurnal patterns of $F_T(h)$ are closely captured in all four periods. *Baldocchi and Meyers* [1998] and *Gu et al.* [1999] also found their model calculations to overestimate $|F_T(h)|$ in the evening. Such a

bias is attributed to the idealization in the terrestrial thermal radiation parameterization and its primitive emissivity formulation.

4.4. Comparison Between Measured and Modeled Mean CO₂ Concentration

In addition to estimating fluxes above the canopy, estimates of CO₂ concentration profiles within the canopy are compared to measurements from the multiport system (Figure 8). Such a comparison permits a unique assessment of the CANVEG model performance to reproduce both spatial and temporal patterns of the mean concentration field, a state variable influenced by the combined source variation and turbulent transport mechanics. In Figure 8 the modeled and measured C_a are contrasted in time (left panels) and in space (right panels) in the canopy for all four periods. The close agreement (see Table 3) between modeled and measured values indicates that the model captures the variation in canopy microclimate temporally and vertically and further supports using the coupled source-dispersion algorithm in the CANVEG model framework.

4.5. Comparison Between Sap Flux Measured and Modeled Bulk Conductance

While eddy covariance flux measurements permit bulk canopy conductance estimates, they are less than optimum for assessing how well leaf-level measurements are integrated to canopy scale by the CANVEG approach. An alternative method is to quantify the pine conductance from sap flux and

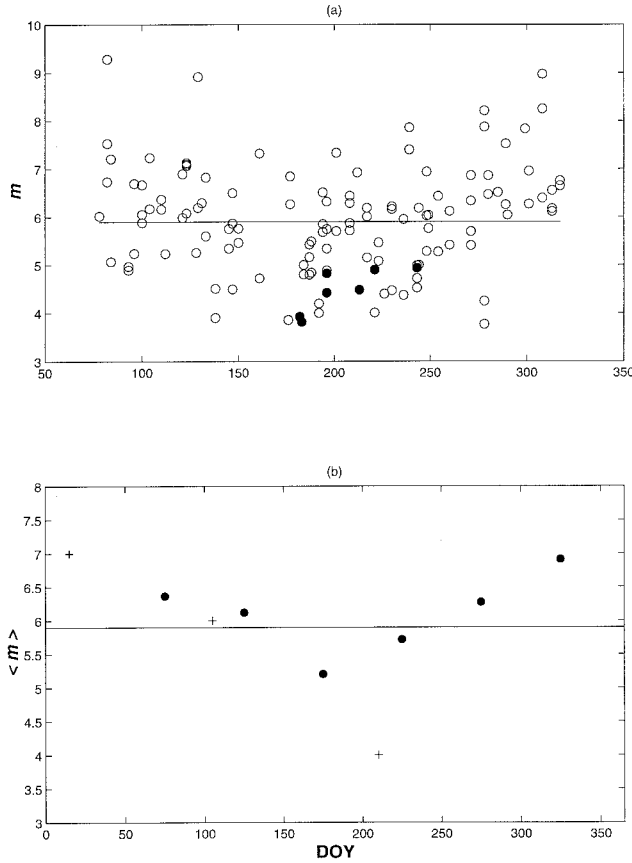


Figure 7. (a) Slope parameter m in the Ball-Berry formulation estimated from porometry measurements over a 3-year period. The m values collected during drought periods are in solid circles. (b) Ensemble means of m values (solid circles) as a function of day of year (DOY) for the 3-year measurement period. The plus symbols are m values determined from the sensitivity analysis for periods 1, 2, and 4, as shown in Table 4. For both panels, the solid line represents the long-term-averaged m ($= 5.9$) determined from the regression analysis in Figure 3.

to contrast these estimates with the pine canopy conductance modeled by the CANVEG based on the pine leaf area and physiological properties.

To compute the bulk canopy conductance (G_c) from the measured E_c , the formulation described by Monteith and Unsworth [1990] and Phillips and Oren [1998] is used and is given by

$$G_c = \frac{\gamma(T_a) \cdot \lambda(T_a) \cdot E_c}{C_p \cdot \rho(T_a) \cdot D_a}, \quad (11)$$

where γ is the psychrometric constant (kPa K^{-1}), λ is the latent heat of vaporization of water, C_p is the specific heat of water, and D_a is the vapor pressure deficit defined as $e_a^*(T_a) - e(T_a)$, where e_a^* and e are the saturation and actual vapor pressure at T_a . Ewers and Oren [2000] demonstrated that for small D_a , G_c estimates from (11) may contain large measurement errors. They suggested a threshold $D_a \geq 0.6$ kPa when computing G_c to keep conductance errors to $<10\%$; their recommended threshold for D_a is used when estimating G_c .

The CANVEG model does not compute bulk canopy conductance directly and hence must be inferred from modeled

conductance at each canopy layer. In the absence of a storage flux, these individual conductance calculations are related to the bulk canopy conductance, after integrating (1), by

$$\begin{aligned} F_{\text{H}_2\text{O}}(h) - F_{\text{H}_2\text{O}}(0) &= G_m D = \int_0^h S_{\text{H}_2\text{O}} dz \\ &= \int_0^h a(z) \frac{e^*(z) - e(z)}{r_s(z) + r_b(z)} dz, \end{aligned} \quad (12)$$

where G_m is the modeled bulk canopy conductance to water vapor, e^* is the saturation vapor pressure at T_s , and D is the vapor pressure deficit calculated by $e^*(T_s) - e(T_a)$. If $D \approx D_a$ and $dD/dz \approx 0$, and assuming that $r_b \ll r_s$, a parallel resistor analogy can then be derived for G_m :

$$G_m \approx \sum_{i=1}^N \frac{a(z_i)}{r_s(z_i)} \cdot \Delta z, \quad (13)$$

where

$$z_{i+1} = z_i + \Delta z, \quad i=1, \dots, N-1. \quad (14)$$

For using the parallel resistor analogy, we selected runs in which D modeled with CANVEG did not vary vertically by more than 5%. In fact, for the majority of daytime runs, the modeled vertical variation of D within the canopy rarely exceeded 5%, as was shown in another loblolly pine plantation of a similar total PAI [Ewers and Oren, 2000].

We note that G_m and G_c are computed with D and D_a , respectively, as a driving force for transpiration. We regressed D with D_a and found that for conductance calculations the approximation $D \approx D_a$ is reasonable (see Table 3). This simplification has also been verified from measurements made in another loblolly pine stand of a similar PAI [Ewers and Oren, 2000]. Figure 9 shows the comparison between G_m and G_c for all four periods. In period 1 (drought condition), G_c was compared with G_m adjusting for w_r , which improved the comparison by $\sim 26\%$ over a comparison that does not correct G_m by w_r for low soil moisture (see Table 3). For the two nonstress periods, modeled G_m was reasonably close to G_c , with period 4 as a notable exception. The scatter in these conductance comparisons may be related to the difficulty in estimating bulk canopy conductance of a forest from sap flux measurements conducted at the base of individual trees [Phillips *et al.*, 1997; Oren *et al.*, 1998b].

Despite the uncertainty in model calculations and sap flux measurements, the overall agreement between measured and modeled bulk canopy conductance is reasonable. Such agreement suggests that the parallel resistor analogy in (13) is appropriate to derive bulk canopy conductance from leaf-level conductance for water vapor if the vapor pressure deficit is nearly uniform within the canopy volume. Whether such an analogy exists for CO₂ is discussed in the following section, particularly with regard to the vertical variation in $C_a - C_i$ or C_i/C_a .

4.6. Comparison of Modeled and Measured Intercellular CO₂ Concentration

After testing the capability of this version of the CANVEG model to reproduce mass and momentum fluxes and scalar concentrations above and within the canopy, we calculated

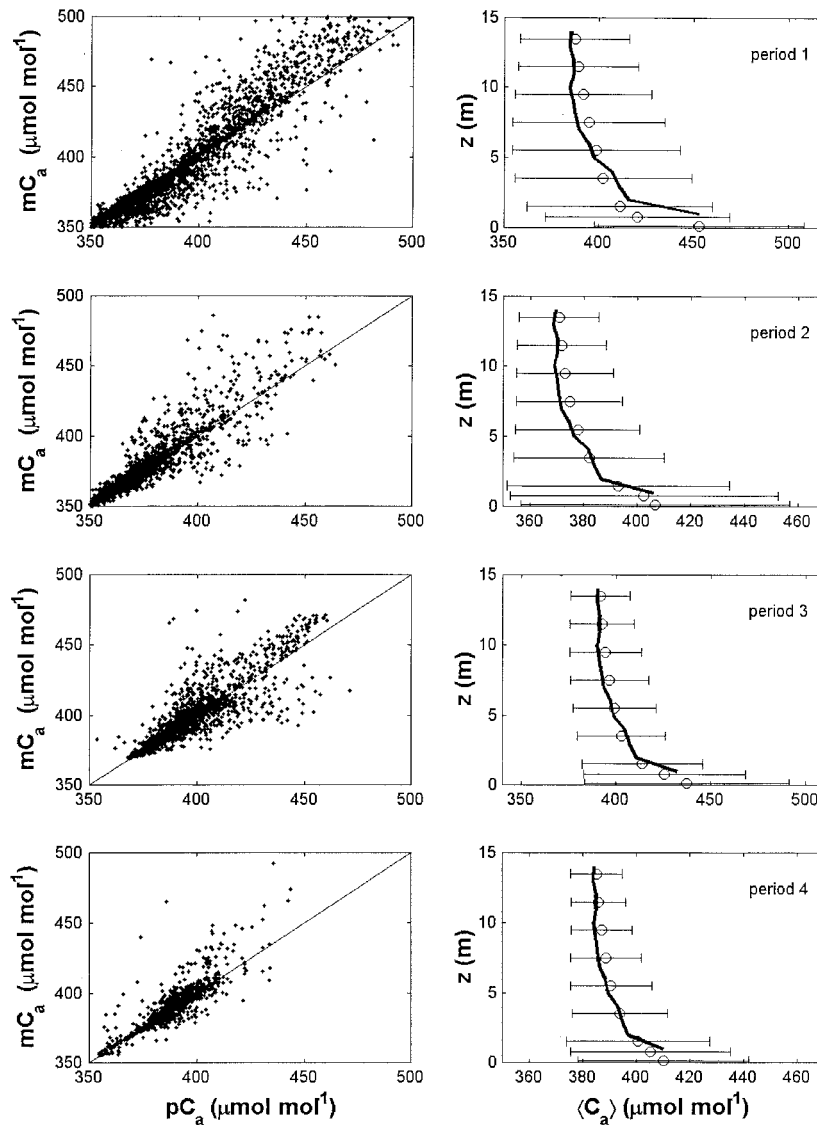


Figure 8. Temporal (left column) and spatial (right column) comparisons between measured (mC_a) and CANVEG-predicted (pC_a) CO₂ concentration variation. For the spatial comparison the ensemble modeled $\langle C_a \rangle$ for each period is the solid line, while the ensemble measurements are plotted as open circles with one standard deviation.

C_i/C_a profiles and compared these estimations with long-term isotope carbon measurements collected on sunlit and shaded foliage, the two expected end members of the range in C_i/C_a . Figure 10 shows the ensemble average of modeled C_i/C_a profiles at three selected layers (5.5, 7.5, and 13.5 m) for the four periods. Also shown is the C_i/C_a value obtained from carbon isotope measurements representing the C_i/C_a integral over the life of leaves, along with porometry measurements on sunlit foliage only averaged for each of the respective months [Ellsworth, 1999, 2000].

The carbon isotope measurements showed that C_i/C_a varied between 0.66 to 0.75 from the top of the canopy to its bottom, while the porometry measurement of sunlit foliage suggested a lower value (as low as 0.56). The modeled C_i/C_a at the canopy top agrees with the $^{13}\delta C$ measurements for midday hours (Figure 10). The modeled C_i/C_a at the lower layers are higher but also consistent with the $^{13}\delta C$ measurements (≈ 0.75) of shaded foliage values. The best agreement occurred in period

2, when temperature and soil moisture did not limit stomatal conductance. The porometry measurements set the lowest C_i/C_a limit for the upper canopy layers. As expected, the modeled C_i/C_a values are marginally higher because they represent integrated sunlit and shaded fractions within each canopy layer. The observed vertical variations in C_i/C_a are consistent with findings in other forests [Weber and Gates, 1990; Yoder *et al.*, 1994; Williams *et al.*, 1996].

The broader implication of vertical variability in C_i/C_a , and its dependence on environmental conditions, is that an “effective” C_i/C_a in “big-leaf” models is ambiguously defined. Therefore compressing photosynthesis parameters in bulk canopy models is likely to increase the uncertainty in CO₂ flux predictions, or worse, inject a systematic bias. We next investigated the impact on the modeled fluxes if big-leaf (or single layer) formulations are adopted. We focused on periods 2 and 3 that reflected the weakest and strongest degree of vertical variation in C_i/C_a with depth.

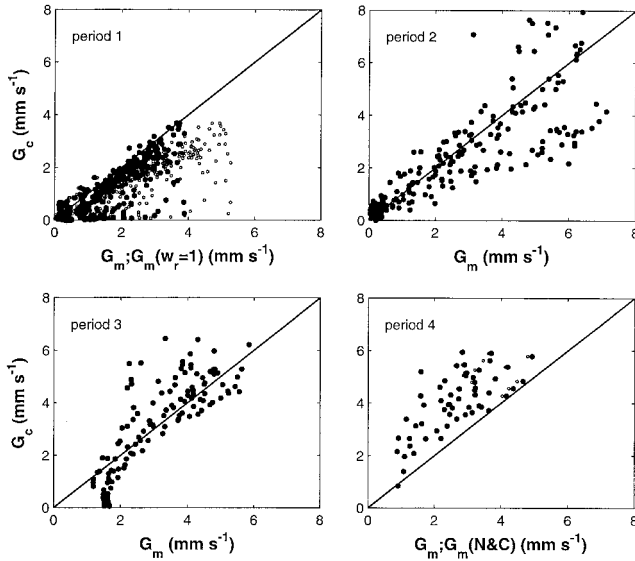


Figure 9. Comparison between modeled conductance (G_m) and sap flux scaled conductance (G_c) of the bulk pine canopy for all four periods. For period 1 (drought), dots and open circles represent the modeled G_m with and without w_r correction, respectively. For period 4 (low temperature) the open circles and dots represent the modeled G_m with $V_{c \max} - T_s$ curve derived from *Campbell and Norman* [1998] and measured on loblolly pine, respectively. The 1:1 line (solid line) is also shown.

For a single layer (or big leaf) whose conductance is identical to the bulk canopy conductance G_m derived in section 4.5, the net assimilation is given by

$$A_n = G_m \overline{(C_a - C_i)} = G_m \overline{C_a} \left(1 - \frac{\overline{C_i}}{\overline{C_a}} \right),$$

where the overbar represents depth averaging. The canopy CO₂ flux from this single layer can be estimated from

$$F_{\text{CO}_2} = A_n - R_d - F_g$$

if R_d and F_g are known, where $\overline{C_a - C_i}$ is the effective $C_a - C_i$ of the big leaf, R_d is the plant respiration and F_g is the soil CO₂ efflux. One approach to estimating $\overline{C_a - C_i}$ is to rearrange the Ball-Berry model as

$$\frac{\overline{C_i}}{\overline{C_a}} \approx 1 - \frac{1}{mrh}.$$

This approximation naturally leads to a constant C_i/C_a with depth within the canopy volume but not with time. Using G_m , R_d , and F_g modeled with CANVEG, we estimated F_{CO_2} for periods 2 and 3 and contrast these calculations with both measurements and calculations with the full CANVEG model. We restate that the only difference in calculating F_{CO_2} between the big-leaf and the detailed multilevel CANVEG model is the vertical variation in C_i/C_a as the driving force for the bulk canopy assimilation. The comparison between modeled F_{CO_2} based on the big-leaf approach and the multilayer CANVEG model, along with measured F_{CO_2} from eddy covariance is shown in Figure 11 for both periods.

The F_{CO_2} computed by the big-leaf approach continuously overestimated the values predicted by the full CANVEG model (Figure 11) with larger divergence between the two approaches in period 3 (regression slopes differed by 10% for period 2 and 30% for period 3). Predictably, when the gradients in C_i/C_a are large, a consistent divergence between CANVEG and big-leaf flux estimates is produced. However, if the root-mean-square error is used as the benchmark for comparisons, then the big-leaf approach is comparable to the CANVEG model calculations. This, in part, is due to the fact that temporal patterns of G_s vary by an order of magnitude, while the vertical variation in C_i/C_a is of the order of 15–25%,

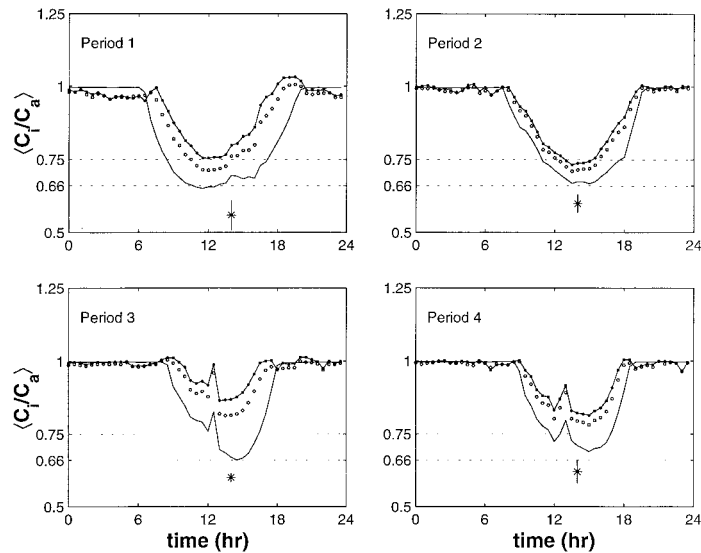


Figure 10. Modeled diurnal C_i/C_a variation at three selected canopy layers ($z = 5.5, 7.5,$ and 13.5 m, represented by dotted line, open circles, and solid line, respectively) for the four periods. The horizontal dashed lines are the long-term carbon isotope measurement at the top (≈ 0.66) and bottom (≈ 0.75) of the canopy [Ellsworth, 1999]. The ensemble leaf-level measurements [Ellsworth, 2000], collected around noon for sunlit foliage only, is shown by a star with one standard deviation.

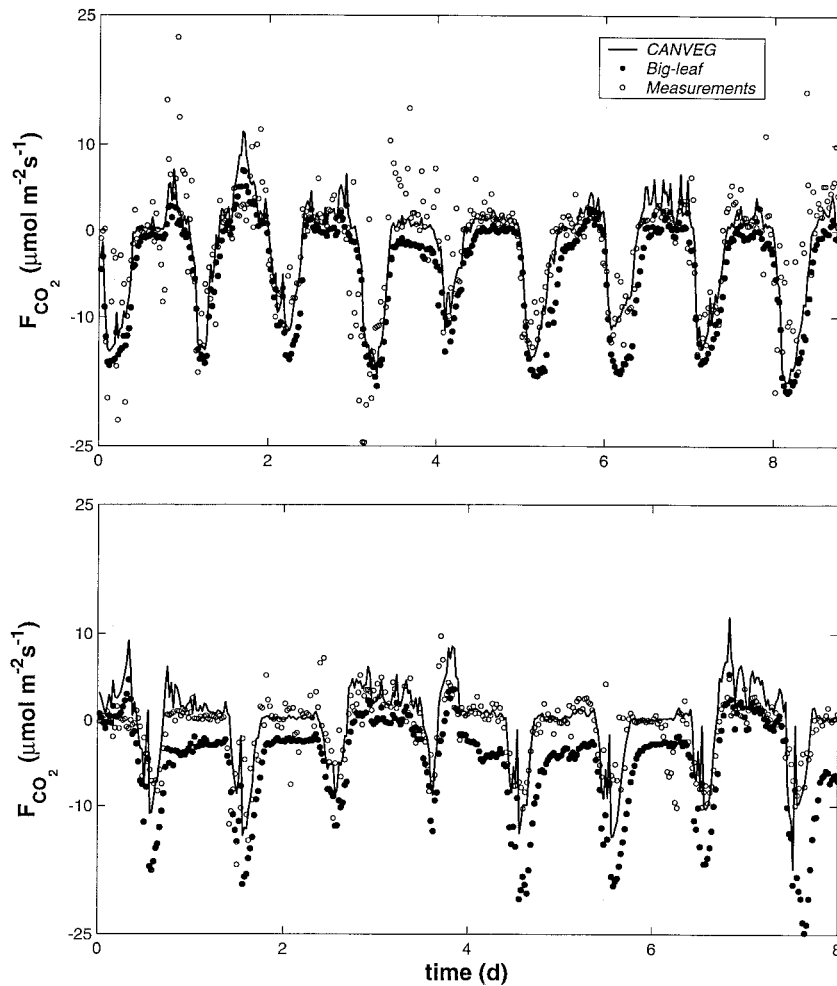


Figure 11. Comparison between F_{CO_2} values estimated based on big leaf (dots) versus CANVEG (solid line) in period 2 (top) and period 3 (bottom), representing small and large vertical variations in modeled C_i/C_a with CANVEG, respectively. The measured F_{CO_2} is also shown by open circles.

meaning that accurate modeling of conductance in time is much more critical to predicting canopy F_{CO_2} than resolving the detailed vertical variation in C_i/C_a .

5. Conclusion

We presented an Eulerian-Lagrangian CANVEG framework that combines micrometeorological, biophysical, and biochemical principles with canopy turbulent transport theory for a wide range of temperature and soil moisture conditions. Modeled CO₂, H₂O, and sensible heat fluxes above the canopy, and CO₂ concentration within the canopy were reasonably close to measurements. In addition, modeled bulk canopy conductance compared well with the canopy conductance derived from scaled sap flux measurements for pine trees. On the basis of these results we conclude the following:

1. The generic temperature correction of the kinetic coefficients reported by *Campbell and Norman* [1998] is different from the locally derived correction for pine foliage. However, the overall CANVEG performance is not sensitive to such difference.
2. The CANVEG framework overestimates H₂O fluxes and bulk canopy conductance without soil moisture adjustment when low soil moisture regulates stomatal conductance.
3. While our proposed reduction function significantly im-

proved the water vapor flux and canopy conductance, the CO₂ flux was not improved. Sensitivity analysis, in conjunction with leaf-level measurements, demonstrated that assuming static physiological parameters is overly simplistic and can inject systematic biases in modeling CO₂ fluxes.

4. Close agreement between the modeled bulk canopy conductance and the sap flux-scaled canopy conductance demonstrates that the parallel resistor analogy is an appropriate scheme to scale leaf conductance to the canopy scale for water vapor, when the vapor pressure deficit is nearly constant inside the canopy. The “big-leaf” canopy conductance is therefore appropriate for estimating stand transpiration.

5. The equivalent “big-leaf” approach for CO₂ was also investigated by showing that vertical variation in C_i/C_a , a parameter driving photosynthesis, is large within the canopy (at least when compared to vapor pressure deficit). Compressing vertical variation of physiological responses to canopy microclimate into “effective canopy” properties can induce systematic biases in CO₂ flux estimates. However, the estimated CO₂ fluxes did not differ between the multilayer CANVEG and the single-layer approximation (in terms of RMSE), because variations in G_s are an order of magnitude larger than the vertical variations in C_i/C_a .

Appendix A: Model of *Farquhar et al.* [1980] and Temperature Adjustments

Using the models of *Farquhar et al.* [1980] and *Collatz et al.* [1991], the net photosynthetic rate at the leaf scale depends on light, CO₂, and leaf temperature and can be described as

$$A_n \approx \min \left\{ \begin{array}{l} J_E \\ J_C \\ J_S \end{array} \right\} - R_d, \quad (\text{A1})$$

where J_E , J_C , and J_S are the assimilation rate restricted by light, ribulose biphosphate (R_u BP) carboxylase (or Rubisco), and the export rate of synthesized sucrose, respectively, and R_d is the respiration rate during the day but in the absence of photorespiration. Photorespiration is treated separately in the model parameterization. The gross assimilation rate ($= A_n + R_d$) is determined by the lowest of the three capacities since no photosynthesis can occur if the supply of any component is insufficient. In (A1), J_E describes the dependence of photosynthesis on light using

$$J_E = \alpha_p \times e_m \times Q_p \frac{\bar{C}_i - \Gamma_*}{\bar{C}_i + 2\Gamma_*}, \quad (\text{A2})$$

where α_p is the leaf absorptivity for PAR, e_m is the maximum quantum efficiency for CO₂ uptake, Q_p is the PAR irradiance on the leaf, \bar{C} represents mean CO₂ concentration, and Γ_* , the CO₂ compensation point, is the CO₂ concentration at which $A_n = 0$ in the absence of photorespiration and is given by

$$\Gamma_* = \frac{[\text{O}_2]}{2\omega}, \quad (\text{A3})$$

where $[\text{O}_2]$ is the oxygen concentration in air (≈ 210 mmol mol⁻¹), and ω is a ratio of kinetic parameters describing the partitioning of R_u BP to the carboxylase or oxygenase reactions of Rubisco. In other words, ω is a measure of the competition between CO₂ and O₂ for R_u BP that is intrinsic to the Rubisco enzyme in C₃ species.

J_C is the Rubisco-limited rate and is estimated from

$$J_C = \frac{V_{c \max}(\bar{C}_i - \Gamma_*)}{\bar{C}_i + K_c(1 + [\text{O}_2]/K_o)}, \quad (\text{A4})$$

where $V_{c \max}$ is the maximum catalytic capacity of Rubisco per unit leaf area ($\mu\text{mol m}^{-2} \text{s}^{-1}$), K_c and K_o are the Michaelis constants for CO₂ fixation and O₂ inhibition with respect to CO₂, respectively. Equation (A4) shows that J_C increases linearly with increasing \bar{C}_i but approaches a maximum value at $V_{c \max}$ under high CO₂ concentration conditions that are generally not encountered under natural conditions.

J_S is the capacity for the export or utilization of photosynthesis products, and sucrose synthesis is most probably the rate-limiting step [see *Collatz et al.*, 1991]. J_S is estimated by

$$J_S = V_{c \max}/2. \quad (\text{A5})$$

The rapid cutoff transition implied in (A1) can be made more realistic if the mathematical scheme is made to account for gradual transition from one limitation to another and to allow for some colimitation among J_E , J_C , and J_S . We used the quadratic functions described by *Collatz et al.* [1991] to circumvent these limitations (not shown here).

We assume that the respiration rate R_d in (A1) is linearly related to $V_{c \max}$ [*Collatz et al.*, 1991] by

$$R_d = 0.015V_{c \max}. \quad (\text{A6})$$

The parameterization of model kinetic variables in terms of temperature dependence follows the procedure of *Campbell and Norman* [1998], in which five parameters are adjusted for temperature: K_c , K_o , ω , $V_{c \max}$, and R_d . For the first three parameters, a modified Q_{10} temperature function is employed:

$$k = k_{25} \exp [y(T_s - 25)], \quad (\text{A7})$$

where k is defined at leaf surface temperature T_s , k_{25} is the value of the parameter at 25°C, and y is the temperature coefficient for that parameter from *Campbell and Norman* [1998]. In addition, $V_{c \max}$ and R_d are adjusted by a more complex function incorporating deactivation effects at extremely high temperatures:

$$V_{c \max} = \frac{V_{c \max,25} \exp [a_1(T_s - 25)]}{1 + \exp [a_2(T_s - 41)]}, \quad (\text{A8})$$

$$R_d = \frac{R_{d,25} \exp [0.069(T_s - 25)]}{1 + \exp [1.3(T_s - 55)]}, \quad (\text{A9})$$

where $V_{c \max,25}$ and $R_{d,25}$ are the values of $V_{c \max}$ and R_d at 25°C, respectively. For (A8), *Campbell and Norman* [1998] reported $a_1 = 0.088$ and $a_2 = 0.29$. Our measured values specifically for pine are $a_1 = 0.051$ and $a_2 = 0.205$.

Finally, \bar{C}_s , \bar{C}_i , and \bar{C}_a are related by

$$\bar{C}_i = \bar{C}_s - \frac{A_n}{g_s}, \quad (\text{A10})$$

$$\bar{C}_s = \bar{C}_a - \frac{A_n}{g_b}, \quad (\text{A11})$$

where g_s ($= r_s^{-1}$) is the stomatal conductance, and g_b ($= r_b^{-1}$) is the leaf boundary layer conductance.

Acknowledgments. The authors thank Yavor Parashkevov and Andrew Palmiotti, for their help during the experiment, and Keith Lewin and John Nagy for their assistance in the CO₂/H₂O multipoint design and setup. This project was funded, in part, by the National Science Foundation (NSF-BIR 12333), and the U.S. Department of Energy (DOE) through the FACE-FACTS project, and through the Southeast Regional Center at the University of Alabama, Tuscaloosa (DOE cooperative agreement DE-FC030-90ER61010), and the National Institute for Global Environmental Change (NIGEC).

References

- Abdella, K., and N. McFarlane, A new second-order turbulence closure scheme for the planetary boundary layer, *J. Atmos. Sci.*, *54*, 1850–1867, 1997.
- Aber, J. D., P. B. Reich, and M. L. Goulden, Extrapolating leaf CO₂ exchange to the canopy: A generalized model of forest photosynthesis compared with measurements by eddy correlation, *Oecologia*, *106*, 257–265, 1996.
- Amthor, J. S., M. L. Goulden, J. W. Munger, and S. C. Wofsy, Testing a mechanistic model of forest-canopy mass and energy exchange using eddy correlation: Carbon dioxide and ozone uptake by a mixed oak-maple stand, *Aust. J. Plant Physiol.*, *21*, 623–651, 1994.
- Andren, A., Evaluation of a turbulence closure scheme suitable for air pollution applications, *J. Appl. Meteorol.*, *29*, 224–239, 1990.
- Baldocchi, D. D., A Lagrangian random-walk model for simulating water vapor, CO₂ and sensible heat flux densities and scalar profiles over and within a soybean canopy, *Boundary Layer Meteorol.*, *61*, 113–144, 1992.

- Baldocchi, D. D., Measuring and modelling carbon dioxide and water vapour exchange over a temperate broad-leaved forest during the 1995 summer drought, *Plant Cell Environ.*, *20*, 1108–1122, 1997.
- Baldocchi, D. D., and T. Meyers, On using eco-physiological, micrometeorological and biogeochemical theory to evaluate carbon dioxide, water vapor and trace gas fluxes over vegetation: A perspective, *Agric. For. Meteorol.*, *90*, 1–25, 1998.
- Baldocchi, D. D., and P. C. Harley, Scaling carbon dioxide and water vapour exchange from leaf to canopy in a deciduous forest: Modeling testing and application, *Plant Cell Environ.*, *18*, 1157–1173, 1995.
- Baldocchi, D. D., C. A. Vogel, and B. Hall, Seasonal variation of carbon dioxide exchange rates above and below a boreal jack pine forest, *Agric. For. Meteorol.*, *83*, 147–170, 1997a.
- Baldocchi, D. D., C. A. Vogel, and B. Hall, Seasonal variation of energy and water vapor exchange rates above and below a boreal jack pine forest canopy, *J. Geophys. Res.*, *102*, 28,939–28,951, 1997b.
- Ball, J. T., I. E. Woodrow, and J. A. Berry, A model predicting stomatal conductance and its contribution to the control of photosynthesis under different environmental conditions, in *Progress in Photosynthesis Research*, edited by J. Biggens, pp. 221–224, Martinus Nijhoff, CZ Zoetermeer, Netherlands, 1987.
- Björkman, O., The response of photosynthesis to temperature, in *Plants and Their Atmospheric Environment*, edited by J. Grace, E. D. Ford, and P. G. Jarvis, pp. 273–302, Blackwell Sci., Malden, Mass., 1981.
- Campbell, G. S., and J. M. Norman, *An Introduction to Environmental Biophysics*, Springer-Verlag, New York, 1998.
- Canuto, V. M., F. Minotti, C. Ronchi, R. M. Ypma, and O. Zeman, Second-order closure PBL model with new third-order moments: Comparison with LES data, *J. Atmos. Sci.*, *51*, 1605–1618, 1994.
- Collatz, G. J., J. T. Ball, C. Grivet, and J. A. Berry, Physiological and environmental regulation of stomatal conductance, photosynthesis and transpiration: A model that includes a laminar boundary layer, *Agric. For. Meteorol.*, *54*, 107–136, 1991.
- Cornic, G., Drought stress and high light effects on leaf photosynthesis, in *Photoinhibition of Photosynthesis From Molecular to the Field*, edited by N. R. Baker and J. R. Bowyer, pp. 297–313, BIOS Sci., Oxford, England, 1994.
- De Pury, D. G. G., and G. D. Farquhar, Simple scaling of photosynthesis from leaves to canopies without the errors of big-leaf models, *Plant Cell Environ.*, *20*, 537–557, 1997.
- Donaldson, C. Du P., Construction of a dynamic model for the production of atmospheric turbulence and the dispersion of atmospheric pollutants, in *Workshop on Micrometeorology*, pp. 313–392, Am. Meteorol. Soc., Boston, Mass., 1973.
- Ellsworth, D. S., CO₂ Enrichment in a maturing pine forest: Are CO₂ exchange and water status in the canopy affected?, *Plant Cell Environ.*, *22*, 461–472, 1999.
- Ellsworth, D. S., Seasonal CO₂ assimilation and stomatal limitations in a *Pinus Taeda* canopy, *Tree Physiol.*, *20*, 435–445, 2000.
- Ewers, B. E., and R. Oren, Analyses of assumptions and errors in the calculation of stomatal conductance from sap flux measurements, *Tree Physiol.*, *20*, 579–589, 2000.
- Ewers, B. E., R. Oren, and J. S. Sperry, Influence of nutrient versus water supply on hydraulic architecture and water balance in *Pinus taeda*, *Plant Cell Environ.*, in press, 2000.
- Fan, S.-M., M. L. Goulden, J. W. Munger, B. C. Daube, P. S. Bakwin, S. C. Wofsy, J. S. Amthor, D. R. Fitzjarrald, K. E. Moore, and T. R. Moore, Environmental controls on the photosynthesis and respiration of a boreal lichen woodland: A growing season of whole-ecosystem exchange measurements by eddy correlation, *Oecologia*, *102*, 443–452, 1995.
- Farquhar, G. D., S. Von Caemmerer, and J. A. Berry, A biochemical model of photosynthetic CO₂ assimilation in leaves of C₃ species, *Planta*, *149*, 78–90, 1980.
- Gollan, T., J. B. Passioura, and R. Munns, Soil water status affects the stomatal conductance of fully turgid wheat and sunflower leaves, *Aust. J. Plant Physiol.*, *13*, 459–464, 1986.
- Grace, J., J. Lloyd, J. McIntyre, A. Miranda, P. Meir, H. Miranda, J. Moncrieff, J. Massheder, I. Wright, and J. Gash, Fluxes of carbon dioxide and water vapour over an undisturbed tropical forest in south-west Amazonia, *Global Change Biol.*, *1*, 1–12, 1995.
- Granier, A., Evaluation of transpiration in a Douglas fir stand by means of sap flow measurements, *Tree Physiol.*, *3*, 309–320, 1987.
- Gu, L., H. H. Shugart, J. D. Fuentes, T. A. Black, and S. R. Shewchuk, Micrometeorology, biophysical exchanges and NEE decomposition in a two-story boreal forest—Development and test of an integrated model, *Agric. For. Meteorol.*, *94*, 123–148, 1999.
- Hacke, U. G., J. S. Sperry, B. E. Ewers, K. V. R. Schäfer, R. Oren, and D. S. Ellsworth, Influence of soil porosity on water use in *Pinus taeda*, *Oecologia*, *24*, 495–505, 2000.
- Harley, P. C., and D. D. Baldocchi, Scaling carbon dioxide and water vapour exchange from leaf to canopy in a deciduous forest, I, Leaf model parameterization, *Plant Cell Environ.*, *18*, 1146–1156, 1995.
- Harley, P. C., and J. D. Tenhunen, Modeling the photosynthetic response of C₃ leaves to environmental factors, in *Modeling photosynthesis—From Biochemistry to Canopy*, edited by K. Boote and R. Loomis, pp. 17–39, Am. Soc. of Agron., Madison, Wis., 1991.
- Harley, P. C., J. A. Weber, and D. M. Gates, Interactive effects of light, leaf temperature, CO₂ and O₂ on photosynthesis in soybean, *Planta*, *165*, 249–263, 1985.
- Harley, P. C., R. B. Thomas, J. F. Reynolds, and B. R. Strain, Modeling photosynthesis of cotton grown in elevated CO₂, *Plant Cell Environ.*, *15*, 271–282, 1992.
- Hinckley, T. M., R. G. Aslin, R. R. Aubuchon, C. L. Metcalf, and J. E. Roberts, Leaf conductance and photosynthesis in four species of the oak-hickory forest type, *For. Sci.*, *24*, 73–84, 1978.
- Hollinger, D. Y., F. M. Kelliher, J. N. Byers, J. E. Hunt, T. M. McSevny, and P. L. Weir, Carbon dioxide exchange between an undisturbed old-growth temperate forest and the atmosphere, *Ecology*, *75*(1), 134–150, 1994.
- Johnson, I. R., and J. H. M. Thornley, Temperature dependence of plants and crop processes, *Ann. Bot.*, *55*, 1–24, 1985.
- Kaimal, J. C., and J. J. Finnigan, *Atmospheric Boundary Layer Flows: Their Structure and Measurements*, 289 pp., Oxford Univ. Press, New York, 1994.
- Katul, G. G., and J. D. Albertson, An investigation of higher order closure models for a forested canopy, *Boundary Layer Meteorol.*, *89*, 47–74, 1998.
- Katul, G. G., and W.-H. Chang, Principal length scales in second-order closure models for canopy turbulence, *J. Appl. Meteorol.*, *38*, 1631–1643, 1999.
- Katul, G. G., R. Oren, D. Ellsworth, C. I. Hsieh, N. Phillips, and K. Lewin, A Lagrangian dispersion model for predicting CO₂ sources, sinks, and fluxes in a uniform loblolly pine (*Pinus taeda* L.) stand, *J. Geophys. Res.*, *102*, 9309–9321, 1997a.
- Katul, G. G., C. I. Hsieh, G. Kuhn, D. Ellsworth, and D. Nie, The turbulent eddy motion at the forest-atmosphere interface, *J. Geophys. Res.*, *102*, 13,409–13,421, 1997b.
- Katul, G. G., et al., Spatial variability of turbulent fluxes in the roughness sublayer of an even-aged pine forest, *Boundary Layer Meteorol.*, *93*, 1–28, 1999.
- Kelliher, F. M., R. Leuning, and E. D. Schulze, Evaporation and canopy characteristics of coniferous forests and grasslands, *Oecologia*, *95*, 153–163, 1993.
- Kramer, P. J., and J. S. Boyer, *Water relations of plants and soils*, Academic, San Diego, Calif., 1995.
- Lai, C.-T., G. Katul, D. S. Ellsworth, and R. Oren, Modeling vegetation-atmosphere CO₂ exchange by a coupled Eulerian-Lagrangian approach, *Boundary Layer Meteorol.*, *95*, 91–12, 2000.
- Lee, X., On micrometeorological observations of surface-air exchange over tall vegetation, *Agric. For. Meteorol.*, *91*, 39–49, 1998.
- Leuning, R., F. M. Kelliher, D. G. G. De Pury, and E.-D. Schulze, Leaf nitrogen, photosynthesis, conductance and transpiration: Scaling from leaves to canopies, *Plant Cell Environ.*, *18*, 1183–1200, 1995.
- Luhar, A. K., and R. E. Britter, A random walk model for dispersion in inhomogeneous turbulence in a convective boundary layer, *Atmos. Environ.*, *23*, 1911–1924, 1989.
- Mellor, G., Analytic prediction of the properties of stratified planetary boundary layer, *J. Atmos. Sci.*, *30*, 1061–1069, 1973.
- Mellor, G. L., and T. Yamada, A hierarchy of turbulence closure models for planetary boundary layers, *J. Atmos. Sci.*, *31*, 1791–1806, 1974.
- Meyers, T. P., and D. D. Baldocchi, The budgets of turbulent kinetic energy and Reynolds stress within and above deciduous forest, *Agric. For. Meteorol.*, *53*, 207–222, 1991.
- Meyers, T. P., and K. T. Paw U, Testing of a higher-order closure model for modeling airflow within and above plant canopies, *Boundary Layer Meteorol.*, *37*, 297–311, 1986.
- Moncrieff, J. B., Y. Malhi, and R. Leuning, The propagation of errors in long-term measurements of land-atmosphere fluxes of carbon and water, *Global Change Biol.*, *2*, 231–240, 1996.

- Monin, A. S., and A. M. Yaglom, *Statistical Fluid Mechanics*, 769 pp., MIT Press, Cambridge, Mass., 1971.
- Monteith, J. L., and M. H. Unsworth, *Principles of Environmental Physics*, pp. 58–259, Edward Arnold, London, 1990.
- Norman, J. M., and J. Welles, Radiative transfer in an array of canopies, *Agron. J.*, **75**, 481–488, 1983.
- Oren, R., B. Ewers, P. Todd, N. Phillips, and G. G. Katul, Water balance delineates the soil layer in which moisture affects canopy conductance, *Ecol. Appl.*, **8**, 990–1002, 1998a.
- Oren R., N. Phillips, G. Katul, B. E. Ewers, and D. E. Pataki, Scaling xylem sap flux and soil water balance and calculating variance: A method for partitioning water flux in forests, *Ann. Sci. For.*, **55**, 191–216, 1998b.
- Pataki, D. E., R. Oren, G. G. Katul, and J. Sigmon, Canopy conductance of *Pinus Taeda*, *Liquidambar Styraciflua*, and *Quercus Phellos* under varying atmospheric and soil water conditions, *Tree Physiol.*, **18**, 307–315, 1998.
- Phillips, N., and R. Oren, A comparison of daily representations of canopy conductance based on two conditional time-averaging methods and the dependence of daily conductance on environmental factors, *Ann. Sci. For.*, **55**, 217–235, 1998.
- Phillips, N., A. Nagchaudhuri, R. Oren, and G. Katul, Time constant for water transport in loblolly pine trees estimated from time series of evaporative demand and stem sapflow, *Tress Struct. Funct.*, **11**(7), 412–419, 1997.
- Raupach, M. R., Canopy transport processes, in *Flow and Transport in the Natural Environment: Advances and Applications*, edited by W. L. Steffen and O. T. Denmead, pp. 95–127, Springer-Verlag, New York, 1988.
- Raupach, M. R., Applying Lagrangian fluid mechanics to infer scalar source distributions from concentration profiles in plant canopies, *Agric. For. Meteorol.*, **47**, 85–108, 1989.
- Raupach, M. R., and R. H. Shaw, Averaging procedures for flow within vegetation canopies, *Boundary Layer Meteorol.*, **22**, 79–90, 1982.
- Sala, A., and J. Tenhunen, Simulations of canopy net photosynthesis and transpiration of *Quercus ilex* L. under the influence of seasonal drought, *Agric. For. Meteorol.*, **78**, 203–222, 1996.
- Schuepp, P. H., Tansley review No. 59: leaf boundary layers, *New Phytol.*, **125**, 477–507, 1993.
- Schulze, E. D., Carbon dioxide and water vapour exchange in response to drought in the atmosphere and in the soil, *Ann. Rev. Plant Physiol.*, **37**, 247–274, 1986.
- Shaw, R. H., Secondary wind speed maxima inside plant canopies, *J. Appl. Meteorol.*, **16**, 514–521, 1977.
- Sperry, J. S., F. R. Adler, G. S. Campbell, and J. P. Comstock, Limitation of plant water use by rhizosphere and xylem conductance: Results from a model, *Plant Cell Environ.*, **21**, 347–359, 1998.
- Tenhunen, J. D., A. Sala Serra, P. C. Harley, R. L. Dougherty, and J. F. Reynolds, Factors influencing carbon fixation and water use by Mediterranean sclerophyll shrubs during summer drought, *Oecologia*, **82**, 381–393, 1990.
- Thomson, D. J., Criteria for the selection of stochastic models of particle trajectories in turbulent flows, *J. Fluid Mech.*, **180**, 529–556, 1987.
- Weber, J. A., and D. M. Gates, Gas exchange in *Quercus rubra* (northern red oak) during a drought: Analysis of relations among photosynthesis, transpiration, and leaf conductance, *Tree Physiol.*, **7**, 215–225, 1990.
- Williams, M., E. B. Rastetter, D. N. Fernandes, M. L. Goulden, S. C. Wofsy, G. R. Shaver, J. M. Meillo, J. W. Munger, S. M. Fan, and K. J. Nadelhoffer, Modeling the soil-plant-atmosphere continuum in a *Quercus-Acer* stand at Harvard Forest: The regulation of stomatal conductance by light, nitrogen and soil/plant hydraulic properties, *Plant Cell Environ.*, **19**, 911–927, 1996.
- Wilson, J. D., A second order closure model for flow through vegetation, *Boundary Layer Meteorol.*, **42**, 371–392, 1988.
- Wilson, J. D., Turbulent transport within the plant canopy, in *Estimation of Areal Evapotranspiration*, 177 pp., *LAHS Publ.*, pp. 43–80, Int. Assoc. of Hydrol. Sci., Gentbrugge, Belgium, 1989.
- Wilson, N. R., and R. H. Shaw, A higher order closure model for canopy flow, *J. Appl. Meteorol.*, **16**, 1198–1205, 1977.
- Wofsy, S. C., M. L. Goulden, J. W. Munger, S.-M. Fan, P. S. Bakwin, B. C. Daube, S. L. Bassow, and F. A. Bazzaz, Net exchange of CO₂ in a mid-latitude forest, *Science*, **260**, 1314–1317, 1993.
- Yoder, B. J., M. G. Ryan, and M. R. Kaufmann, Evidence of reduced photosynthetic rates in old trees, *For. Sci.*, **40**, 513–527, 1994.

D. Ellsworth, Environmental Biology and Instrumentation Division, Brookhaven National Laboratory, Upton, NY 11973-5000, USA.

G. Katul, C.-T. Lai, R. Oren, and K. Schäfer, School of the Environment, Box 90328, Duke University, Durham, NC 27708-0328. (cl9@duke.edu)

(Received December 31, 1999; revised June 8, 2000; accepted July 26, 2000.)

